

The Discovery of I-BET726 (GSK1324726A), a Potent Tetrahydroquinoline ApoA1 Up-Regulator and Selective BET Bromodomain Inhibitor

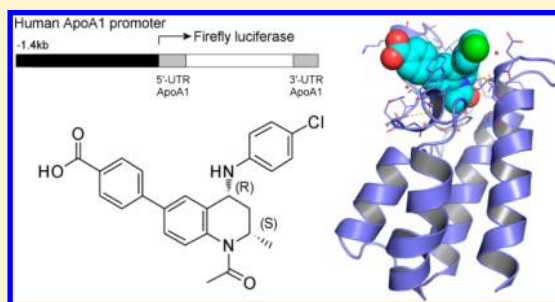
Romain Gosmini,^{†,¶} Van Loc Nguyen,[†] Jérôme Toum,[†] Christophe Simon,^{†,+} Jean-Marie G. Brusq,[‡] Gael Krysa,[‡] Olivier Mirguet,^{†,▲} Alizon M. Riou-Eymard,[‡] Eric V. Boursier,[§] Lionel Trottet,[§] Paul Bamborough,^{*,⊥} Hugh Clark,[○] Chun-wa Chung,[⊥] Leanne Cutler,[#] Emmanuel H. Demont,^{||} Rejbinder Kaur,^{||} Antonia J. Lewis,[∇] Mark B. Schilling,[○] Peter E. Soden,^{||} Simon Taylor,[#] Ann L. Walker,[◆] Matthew D. Walker,[○] Rab K. Prinjha,^{*,||} and Edwige Nicodème[‡]

[†]Candidate Discovery, [‡]Discovery Biology, [§]DMPK, GlaxoSmithKline Les Ulis, Centre de Recherches François Hyafil, GlaxoSmithKline R&D, 25 Avenue du Québec, 91140 Villebon-sur-Yvette, France

^{||}Epinova Discovery Performance Unit, [⊥]Computational & Structural Chemistry, [#]Experimental Medicine Unit, [∇]Biological Sciences, [○]Exploratory Development Sciences, [◆]Discovery Partnerships Medicinal Chemistry, GlaxoSmithKline Stevenage, Medicines Research Centre, Gunnels Wood Road, Stevenage, Hertfordshire SG1 2NY, U.K.

Supporting Information

ABSTRACT: Through their function as epigenetic readers of the histone code, the BET family of bromodomain-containing proteins regulate expression of multiple genes of therapeutic relevance, including those involved in tumor cell growth and inflammation. BET bromodomain inhibitors have profound antiproliferative and anti-inflammatory effects which translate into efficacy in oncology and inflammation models, and the first compounds have now progressed into clinical trials. The exciting biology of the BETs has led to great interest in the discovery of novel inhibitor classes. Here we describe the identification of a novel tetrahydroquinoline series through up-regulation of apolipoprotein A1 and the optimization into potent compounds active in murine models of septic shock and neuroblastoma. At the molecular level, these effects are produced by inhibition of BET bromodomains. X-ray crystallography reveals the interactions explaining the structure–activity relationships of binding. The resulting lead molecule, I-BET726, represents a new, potent, and selective class of tetrahydroquinoline-based BET inhibitors.



INTRODUCTION

Atherosclerosis is a significant cause of mortality, and although currently treated by lipid-modifying drugs such as statins, a need remains for novel treatments. Decreased risk of atherosclerosis is associated with higher levels of high density lipoprotein (HDL) cholesterol. The apolipoprotein A1 protein (ApoA1) is a major component of HDL, and its overexpression is correlated with increased HDL cholesterol levels.^{1,2} ApoA1 up-regulation therefore offers a novel alternative to existing treatments for atherosclerosis, although until quite recently no molecular mechanism to bring that about was known.³

We recently reported the use of a cellular reporter assay to discover novel ApoA1 up-regulators, such as the benzodiazepine (BZD) compounds exemplified by **1** (GSK525762A/I-BET762, Figure 1), which is currently in clinical development.^{4–6} These were shown via chemoproteomics and other approaches to bind to the tandem bromodomains of the bromodomain and extra terminal domain (BET) family proteins and also have potent anti-inflammatory activity.⁷ The

four members of this family, BRD2, BRD3, and BRD4 (together with BRDT, whose expression is restricted to testis and ovary), activate transcription via recognition of the acetylated lysine state of histone tails and other proteins and recruitment of polymerases and transcription factors.^{8,9} Each BET protein contains two bromodomains, modules which specifically recognize the acetylated state of their partners, including the histone protein tails whose acetylation forms part of the histone code of epigenetic gene regulation. Small molecule inhibitors of bromodomain binding to histones have emerged over recent years and are now of great current interest for wide-ranging applications including atherosclerosis, inflammation, and oncology.^{10–13}

A thienotriazolodiazepine with structural similarity to **1**, discovered by a group at Mitsubishi Tanabe as an inhibitor of CD28-dependent T-cell growth and inflammation, was also

Received: July 11, 2014

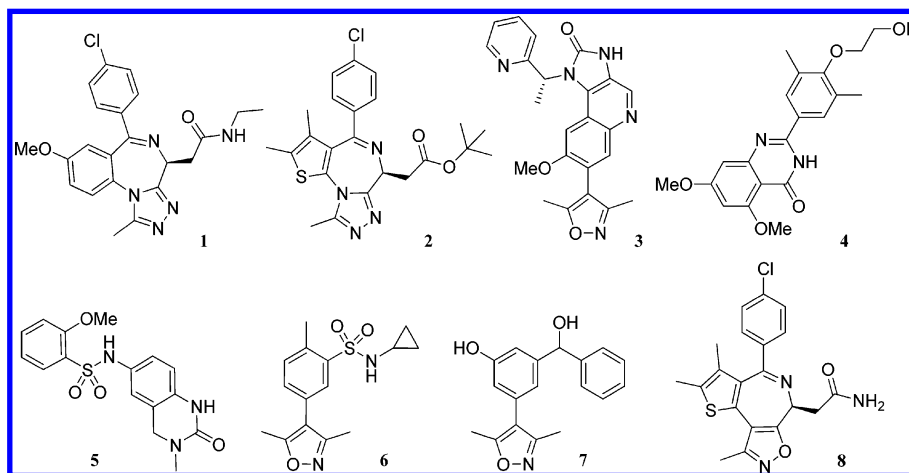


Figure 1. Some examples of BET bromodomain inhibitors, 1–8.

found to target the BET bromodomains.^{14,15} An exemplar of this chemotype, **2** (JQ1), has been released to the worldwide academic community by the Chemical Probe Consortium.¹⁶ This molecule shows strong effects in a range of cancer cell types. For example, NUT midline carcinoma (NMC) is an aggressive tumor in which the BRD4–NUT fusion oncoprotein prevents normal cell differentiation.¹⁷ Treatment of NMC cell lines with **2** halted proliferation and restored normal differentiation.¹⁸ **2** and other BET inhibitors also show effects in models of hematologic cancers (including acute myeloid leukemia, Burkitt's lymphoma, MLL-fusion leukemia, multiple myeloma, and B-cell lymphoblastic leukemia) and neuroblastoma.^{19–23}

Other classes of BET bromodomain inhibitors have been reported. We recently described an unrelated series of quinoline isoxazole ApoA1 up-regulators (e.g., **3**, I-BET151), which also exert their effects through binding to the BET bromodomains.^{24,25} **3** has been investigated for indications including acute leukemia, including MLL-related acute myeloid leukemia, and JAK2-driven myeloproliferative neoplasms.^{20,26} Compound **4** (RVX-208) was also discovered as an ApoA1 up-regulator and has entered clinical trials for atherosclerosis.²⁷ It has since been found that its molecular binding partners include the BET tandem bromodomains.²⁸

Beyond cell-based screening, the BET bromodomains are highly tractable to structure-based and fragment-based drug discovery, taking advantage of increasing understanding of the molecular architecture and binding preferences of the acetyl-lysine site.²⁹ Examples of molecules developed from fragments binding in the AcK site and growing outward to exploit additional binding interactions include the tetrahydroquinolinone **5** (PFI-1), isoxazoles such as **6** and **7**, and compounds incorporating elements of these such as **8**.^{30–35} In this manuscript we describe the discovery of a new series of tetrahydroquinoline-based ApoA1 up-regulators that function through BET inhibition and their optimization to a potent and selective compound active in models of acute inflammation.

RESULTS AND DISCUSSION

Molecular Targets of the Tetrahydroquinolines.

Throughout the optimization work reported here, the molecular mode of action of the tetrahydroquinolines was unknown. In due course, we discovered that other families of ApoA1 up-regulators operate by specific, histone-competitive

binding to the BET family of bromodomain-containing proteins.⁴ We therefore screened representative compounds from the tetrahydroquinoline series in a fluorescence anisotropy (FA) binding assay by measuring the displacement of a ligand from the acetyl-lysine site of recombinant BET bromodomains. As with previously published series of BET inhibitors, BET binding and ApoA1 reporter activation correlate reasonably well, although this is limited by the tight binding limit of the FA assay and factors such as cell permeability.^{4,25} In this article, we show the ApoA1 reporter activation data, which was used to make the decisions that drove lead optimization, alongside the BET bromodomain activity which was gathered later. The Results and Discussion section concludes with X-ray structures showing the binding modes of representative molecules in BRD2 and BRD4, which will be used to rationalize the structure–activity relationships found.

Identification of Tetrahydroquinolines as ApoA1 Up-Regulators. Tetrahydroquinoline **9** (Table 1) was identified from the output of a high-throughput screening campaign as an

Table 1. ApoA1 Luciferase Activation (Fold) of Initial Hits and Analogues after 16 h in HepG2 Cells

| compd | relative stereochemistry ^a | ApoA1 reporter activation | | | |
|-----------|---------------------------------------|---------------------------|----------------|---------|---------|
| | | R ₁ | R ₄ | 1.25 μM | 10 μM |
| 9 | mixture | Me | H | 1.7 | 2.3–3.3 |
| 10 | <i>cis</i> | Me | Me | 1.7 | |
| 11 | <i>trans</i> | Me | Me | 1.1 | |
| 12 | <i>cis</i> | Me | H | 1.7–2.0 | |
| 13 | mixture | Et | H | 1.6 | 1.4–2.9 |
| 14 | mixture | Pr | H | | ≤1.1 |
| 15 | mixture | Bu | H | | ≤1.1 |

^aAll compounds are racemates. “Mixture” indicates a mixture of diastereoisomers.

Table 2. Mean Potency (ApoA1 Luciferase and BET FA) and Solubility of 16–29 (* Denotes Single Enantiomer, Otherwise Racemic Mixtures with *cis* Stereochemistry)

| Compound | R ₄ | R ₆ | ApoA1 pEC ₁₇₀ | BRD2 pIC ₅₀ | BRD3 pIC ₅₀ | BRD4 pIC ₅₀ | Solubility μg/ml |
|----------|----------------|-----------------------------------|-----------------------------|---------------------------|---------------------------|---------------------------|---------------------|
| 16 | Ph | H | 7.0 | 6.1 | 6.3 | 6.1 | |
| 17 | Ph | 4-CN | 7.0 | 6.0 | 6.1 | 6.2 | 57 |
| 18 | Ph | 4-CO ₂ CH ₃ | 7.4 | 5.9 | 6.0 | 5.9 | 69 |
| 19 | Ph | 4-CO ₂ H | 7.3 | 6.2 | 6.4 | 6.3 | 118 |
| 20 | Ph | 4-CF ₃ | 6.2 | 5.7 | 5.9 | 6.0 | |
| 21 | Ph | 4-OMe | 7.2 | 5.9 | 6.2 | 6.2 | 92 |
| 22 | Ph | 4-CH ₂ OH | 7.5 | 6.1 | 6.3 | 6.3 | 73 |
| 23 | Ph | 4-(morpholin-4-ylmethyl) | 7.6 | 6.1 | 6.2 | 6.3 | 107 |
| 24 | Ph | 3-(piperidin-4-ylmethyl) | 7.1 ^a | 5.9 | 6.4 | 6.1 | 99 |
| 25 | Ph | 4-(piperidin-4-ylmethyl) | 7.9 | | | | 111 |
| 26 | CH=O | 4-(piperidin-4-ylmethyl) | 5.3 | 4.8 | 5.2 | 5.2 | |
| 27 | H | 4-(piperidin-4-ylmethyl) | < 5.0 | 4.3 ^a | 4.6 | 4.5 | |
| 28* | Ph | 4-(piperidin-4-ylmethyl) | 8.0 | 6.3 ^a | 6.5 ^a | 6.4 ^a | 125 |
| 29* | Ph | 4-(piperidin-4-ylmethyl) | 5.9 | 4.6 ^a | 4.6 | 4.6 | |

^aSee Supporting Information, Table S1, for standard deviations and other notes.

up-regulator of ApoA1 in the HepG2 cell luciferase reporter assay. At 10 μM, **9** increased luciferase luminescence by 2.2–3.3-fold after 16 h. Because of this promising level of activity, this compound and analogues, which were originally purchased from a commercial vendor as mixtures of undefined stereochemistry, were investigated further. The *para*-methyl analogue was prepared (see Scheme 1, Synthetic Chemistry) and separated into its *cis* and *trans* stereoisomers **10** and **11**. The ApoA1 activation ability of the *cis* isomer **10** was similar to **9**, but its *trans* isomer **11** was inactive (Table 1). The *cis* isomer of **9** was also synthesized, giving **12**, which retained ApoA1 activity. These results strongly suggested that the activity resided in the *cis* stereochemistry.

Initial Exploration at the N1 Position. To understand the effects of modifications at the acetamide position, analogues were first sought within the GSK compound collection. Like **9**, compounds **13**–**15** originated from a commercial supplier. The propionamide analogue **13** retained levels of ApoA1 activity comparable to those of the acetamide **9**, but the butyramide and pentanamide analogues **14** and **15** were inactive. This suggested that further modification of this position was unlikely to be productive. However, the knowledge that SAR existed in modifications at the N1 position as well as in the stereochemistry of the tetrahydroquinolinone core led us to investigate some of the other positions of this template.

Optimization of the 6-Position. The key 6-bromo tetrahydroquinoline intermediate *N*-((2*S**,4*R**)-1-acetyl-6-bromo-2-methyl-1,2,3,4-tetrahydroquinolin-4-yl)formamide (**56**) was used to prepare an initial set of aryl substituted racemic *cis*-stereochemistry analogues through Suzuki chemistry (see Scheme 2, Synthetic Chemistry). The choice of this substituent position was inspired by a pharmacophore model involving the overlay of THQs such as **10** with members of

another series of ApoA1 up-regulators, which will be reported in due course. Introduction of the unsubstituted phenyl ring at the 6-position (R₆ = H, Table 2) yielded **16**, which was found to be a highly potent ApoA1 activator. This encouraged us to make additional substituted analogues. Para substitution of the 6-phenyl ring was well tolerated (**17**–**22**), with polar groups offering some improvement both in activity and solubility. The ring was particularly tolerant of highly polar functionality, for example the carboxylic acid (**19**). Interestingly, the acid substituent at this position did not negatively impact the cellular activity of the molecule (compare the acid **19** to its methyl ester **18**).

Because of the tolerance of charged functionality on this ring, a range of sizable substituents with varying degrees of basicity (morpholine, piperazine, and piperidine) were prepared, for example **23**–**25**. These substituents were very well tolerated at both 3- and 4- positions of the 6-phenyl ring, giving enhanced solubility and similar small improvements in potency (Table 2).

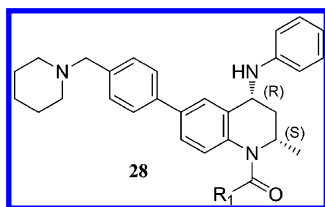
Because of the excellent activity of the piperidine **25**, it was subjected to chiral separation to yield a pair of enantiomers, compounds **28** and **29**. Almost all of the ApoA1 reporter activity resided in one enantiomer, **28**. Although no sample of the racemate (**25**) remained for testing by the time the bromodomain assays were developed, the relative activity of the pair of separated enantiomers in the BET assays mirrored that in the ApoA1 reporter assay. The absolute stereochemistry of the active enantiomer was later shown by X-ray crystallography to be the (2*S*,4*R*) stereoisomer.

Two intermediates (**26** and **27**) prepared en route to **25** (Scheme 4, Synthetic Chemistry) were tested to determine the effect of removing the THQ 4-position aryl substituent. Both were very much weaker in the ApoA1 and BET assays than **25**

or its active enantiomer **28** (Table 2), showing the importance of the 4-anilino substituent for maintaining potency.

Additional properties of **28** are shown in Table 3. Its solubility was good and in vitro clearance in hepatocytes from

Table 3. Some Properties of Compound **28**



| | | 28 |
|---|----------------------|------------------------------|
| peptide-based FRET (pIC ₅₀) | BRD4 | 6.7 ± 0.03 (2) |
| LPS-stimulated IL6 pIC ₅₀ | PBMC | 8.5 ± 0.2 (2) |
| | HWB | 7.2 ± 0.6 (670) ^a |
| FASSIF solubility | μg/mL | 125 |
| hepatocyte clearance (mL/min/g tissue) | human | 1.8 |
| | rat | 0.8 |
| | dog | 0.9 |
| | primate ^b | 6.0 |
| P450 profile IC ₅₀ (μM) | 1A2 (ER) | >33 |
| | 2C9 (FCA) | 14 |
| | 2C19 (BMC) | 20 |
| | 2D6 (MMMC) | 8 |
| | 3A4 (7BQ) | 10 |
| | 3A4 (DEF) | 2 |

^aThis compound was used as a standard in the HWB assay: the mean pIC₅₀ excludes 3 occasions when fitted values could not be obtained.

^bCynomolgous monkey.

three species was low, giving grounds for optimism that the series would have good pharmacokinetic properties. Compound **28** was potent in an alternative BET bromodomain TR-FRET assay measuring displacement of a labeled histone tail peptide. Furthermore, it showed potent anti-inflammatory activity in vitro, as measured by inhibition of the pro-inflammatory cytokine IL6 in LPS-stimulated peripheral blood mononuclear cells (PBMCs) and human whole blood (HWB). However, moderate inhibition of multiple cytochrome P450 isoforms was also found. Because P450 enzymes are involved in the oxidative metabolism of statins, which are widely used for treatment of atherosclerosis, an additional consideration was to minimize any risk of drug–drug interactions by reducing the P450 inhibition of compounds which might be coadministered.³⁶

Our next step was to explore greater diversity at the THQ 4-position. On the basis of the results described above for compounds **18–19**, it was decided to do this first in compounds substituted at the THQ 6-position by *p*-CO₂H phenyl and *p*-CO₂Me phenyl. Para substitution of the THQ 4-anilino ring was well tolerated (Table 4), with even quite sterically bulky groups such as *t*-butyl retaining acceptable activity (**30**). Introduction of groups of similar size but greater polarity such as the methyl sulfone (**31**, **32**) led to some loss of ApoA1 potency. Because the BET activity of **32** was

comparable to the equivalent tertiary butyl **30**, it seems likely that the polarity of **32** negatively impacts its cell permeability. However, the greatest ApoA1 activity was obtained with simple 4-methyl, 4-chloro, or 4-fluoro substituents (**33–35**).

Ortho and meta substitution of the 4-anilino ring was also well tolerated. For example, the 2-OMe analogue (**39**) was comparable to the 3-OMe analogue **38**.

To summarize the above results, the THQ 4-position phenyl ring showed only small substituent effects on BET activity, although more significant differences were seen in cellular ApoA1 up-regulation. Compounds with the 4-chlorophenyl aniline at the THQ 4-position (such as **34**) seemed to offer the best combination of properties and potency. Incorporating this feature, the 6-position was then revisited to explore more diversely substituted phenyls.

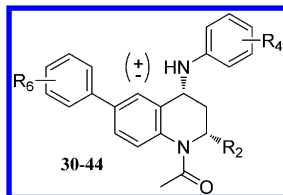
Combining the piperidine-containing 6-aryl group of **25** with the chlorophenyl aniline 4-position of **34** led to **40**, a molecule which, although potent, did not afford an advantage over **25** or **34**. Moving the acid group of **34** from the para to the meta position of the 6-aryl substituent, or replacing it with an ester at the meta position, was slightly detrimental (**41**, **42**). Replacement of the acid by a primary carboxamide (**43**) had little effect. Other positions were rather more sensitive to change, however. For instance, the addition of a small methyl substituent at the ortho position of the THQ 6-phenyl substituent led to a marked reduction of ApoA1 activity (**44**), an observation that was also found later in the BET binding assay.

The THQ 2-methyl group was suspected to be important for activity because of the preference for **28** over its enantiomer **29**. To further assess its significance, an analogue of **21** lacking the 2-methyl substituent (**45**) was prepared and tested. This was weaker than **21** in all assays, confirming that the THQ 2-position methyl substituent does play a role in both ApoA1 induction and BET binding.

After this exploration, the most promising compounds were **33** and **34**, which showed potency comparable to that of **25**. Pure enantiomers of these two compounds (**46**, **47**) were prepared according to Scheme 6, Synthetic Chemistry. These molecules had very similar properties, so **47** (GSK1324726A, I-BET726) was chosen as our leading molecule from this series.

Synthetic Chemistry. Compounds **9** and **13–15** were purchased. All others were synthesized using the general routes shown in Schemes 1–6.⁴⁰ Compounds **10–12** were prepared according to Scheme 1. Aniline was condensed with crotonic acid, giving the Michael addition adduct, which was then cyclized to 2-methyl-2,3-dihydroquinolin-4(1H)-one (**50**) by heating in polyphosphoric acid (PPA) at 110 °C. Following acetylation under standard conditions, reductive amination in the presence of 4-methylaniline and titanium tetrachloride followed by reduction with sodium borohydride gave compounds **10** and **11** as a mixture of *cis*- and *trans*-diastereoisomers. The two isomers were easily separated by flash chromatography.

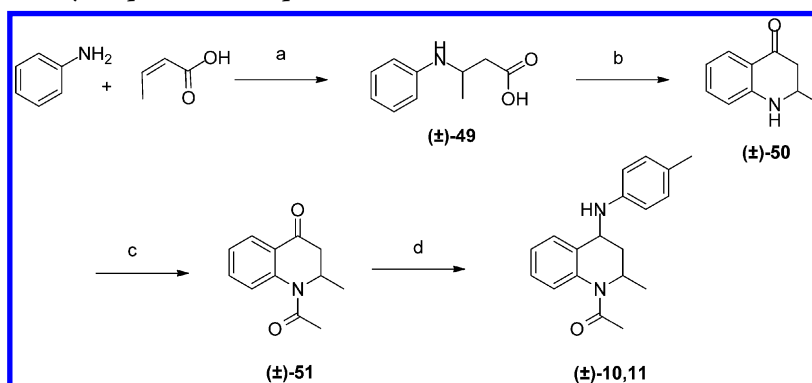
Compounds **16–22**, **36**, **37**, **41**, **42**, and **44** were synthesized according to Scheme 2. 4-Bromoaniline was reacted with acetaldehyde in the presence of benzotriazole in toluene at room temperature. *N*-(1-(1*H*-Benzo[*d*][1,2,3]triazol-1-yl)-ethyl)-4-bromoaniline (**52**) was obtained in modest yield. Reaction with *N*-vinyl formamide in the presence of a Lewis acid such as BF₃·Et₂O in dry THF gave the hetero-Diels–Alder adduct **53** as a racemic *cis*-mixture. The tetrahydroquinoline nitrogen atom was then substituted with an acyl chloride in the

Table 4. Mean Potency of 30–47 in ApoA1 Reporter and BET Bromodomain Assays (*Denotes Single Enantiomer, Otherwise Racemic Mixtures with *cis* Stereochemistry)^a

| Compound | R ₂ | R ₄ | R ₆ | ApoA1 pEC ₁₇₀ | BRD2 pIC ₅₀ | BRD3 pIC ₅₀ | BRD4 pIC ₅₀ |
|----------|----------------|----------------------|--------------------------|-----------------------------|---------------------------|---------------------------|---------------------------|
| 30 | Me | 4-tBu | 4-CO ₂ Me | 6.9 | 6.3 | 6.3 | 6.2 |
| 31 | Me | 4-SO ₂ Me | 4-CO ₂ H | 5.4 | 6.0 | 6.5 | 6.5 |
| 32 | Me | 4-SO ₂ Me | 4-CO ₂ Me | 6.0 | 5.9 | 6.3 | 6.2 |
| 33 | Me | 4-Me | 4-CO ₂ H | 7.8 | 6.3 | 6.5 | 6.2 |
| 34 | Me | 4-Cl | 4-CO ₂ H | 7.8 | 6.4 | 6.4 | 6.3 |
| 35 | Me | 4-F | 4-CO ₂ Me | 7.3 | 5.8 | 6.0 | 6.1 |
| 36 | Me | 3-F | 4-CN | 6.8 | 5.9 | 6.1 | 6.0 |
| 37 | Me | 3-OMe | 4-CN | 6.7 | 5.8 | 6.1 | 6.0 |
| 38 | Me | 3-OMe | 4-CO ₂ H | 7.3 | 6.2 | 6.3 | 6.3 |
| 39 | Me | 2-OMe | 4-CO ₂ H | 7.6 | 6.2 | 6.3 | 6.2 |
| 40 | Me | 4-Cl | 4-(piperidin-2-ylmethyl) | 8.0 | 6.0 | 5.9 | 6.0 |
| 41 | Me | 4-Cl | 3-CO ₂ H | 7.4 | 6.1 | 6.3 | 6.1 |
| 42 | Me | 4-Cl | 3-CO ₂ Me | 7.2 | 5.7 | 6.0 | 6.0 |
| 43 | Me | 4-Cl | 4-CONH ₂ | 7.8 | 6.1 | 6.4 | 6.3 |
| 44 | Me | 4-Cl | 2-Me | 5.6 | 5.4 | 5.6 | 5.4 |
| 45 | H | H | 4-OMe | 6.1 | 5.2 | 5.8 | 5.6 |
| 46* | Me | 4-Me | 4-CO ₂ H | 8.0 | 6.7 | 6.8 | 6.6 |
| 47* | Me | 4-Cl | 4-CO ₂ H | 8.1 | 6.8 | 6.7 | 6.6 |

^aSee Supporting Information Table S2 for standard deviation.

Scheme 1. Synthesis of Tetrahydroquinoline Compounds 10–11^a



^aReagents and conditions: (a) toluene, reflux, 43%; (b) PPA, 110 °C, 29%; (c) AcCl, DMAP, 0 °C to RT, 86%; (d) 4-methylaniline, TiCl₄, TEA, THF/DCM, 0 °C to RT then NaBH₄, RT, 15%.

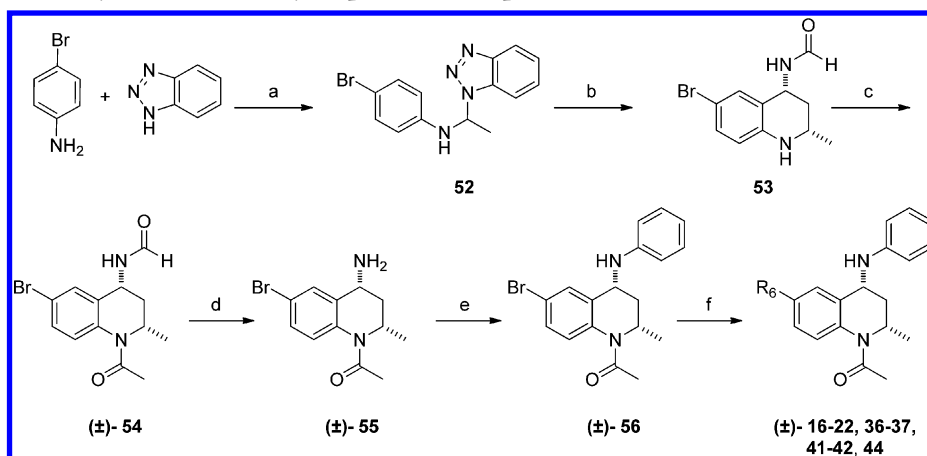
presence of pyridine, giving **54**. The formamide was deprotected using 6 N HCl in refluxing methanol to afford **55**, which reacted with phenylboronic acid under Chan–Lam–Evans conditions. Finally, R₆ was introduced using Suzuki coupling. Tetrahydroquinoline compounds could also be obtained from **54** using the same reagents and conditions in a different order, beginning with the installation of the R₆ substituent, as depicted in Scheme 3.

When the R₆ group bears a hydrophilic basic heterocycle such as piperidine or morpholine, compounds such as **23–26** and **40** could be obtained from intermediate **54** as shown in Scheme 4, beginning with Suzuki coupling with 3- or 4-formylphenylboronic acid. Reductive amination in the presence of the desired cyclic amine and sodium triacetoxyborohydride afforded intermediates of general form **59** which, after

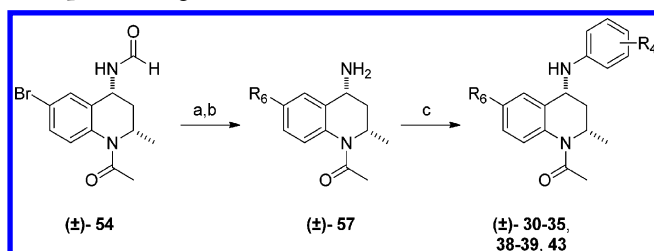
deprotection and copper-mediated Chan–Lam–Evans coupling, gave products **23–25**.

Compound **45**, lacking the tetrahydroquinoline 2-position methyl substituent, was prepared according to Scheme 5. 2,3-Dihydroquinolin-4(1H)-one was brominated at position 6 in the presence of NBS in DCM. The tetrahydroquinoline nitrogen atom was then substituted using an acetic anhydride, giving **61**. A Suzuki coupling reaction was used to introduce the 4-methoxyphenyl substituent at position 6, affording the 6-aryl tetrahydroquinolinon-4-one. Finally, the substituent at position 4 was introduced by reductive amination with aniline in the presence of titanium tetrachloride before reduction with sodium triacetoxyborohydride, giving compound **45**.

47 can also be prepared in an eight-step synthesis starting from isopropyl carbamate. Reaction with crotonyl chloride at –20 °C formed the but-2-enoyl carbamate **63**. An aza-Michael

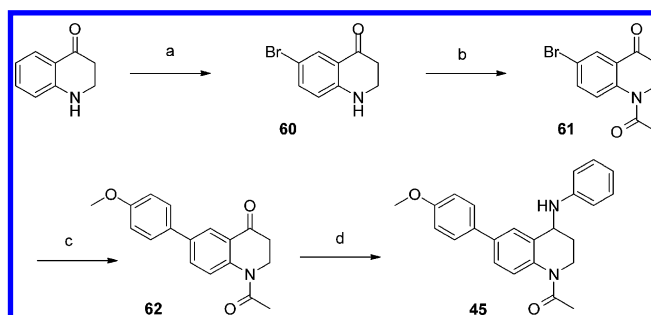
Scheme 2. Representative Synthesis of Tetrahydroquinoline Compounds 16–22, 36–37, 41–42, and 44^a

^aReagents and conditions: (a) MeCHO, toluene, RT, 82%; (b) *N*-vinylformamide, BF₃·Et₂O, THF, -5 °C, 56%; (c) MeCOCl, DCM, pyridine, 0 °C, 100%; (d) MeOH, 6 N HCl, reflux, 91%; (e) PhB(OH)₂, Cu(OAc)₂, TEA, DCM, RT; (f) R₆B(OH)₂, Pd(PPh₃)₄, Na₂CO₃, DME, H₂O, reflux.

Scheme 3. Alternative Synthesis of Tetrahydroquinoline Compounds, e.g., 30–35, 38–39, and 43^a

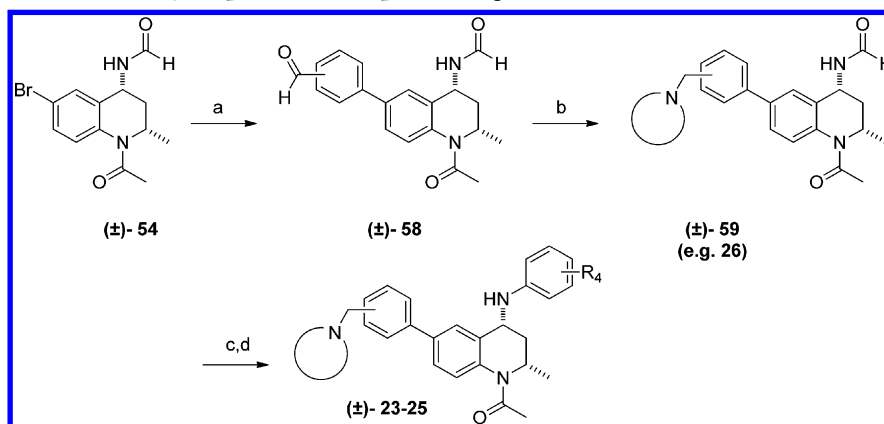
^aReagents and conditions: (a) R₆B(OH)₂, Pd(PPh₃)₄, Na₂CO₃, DME, H₂O, reflux; (b) MeOH, 6 N HCl, reflux; (c) R₆PhB(OH)₂, Cu(OAc)₂, TEA, DCM, RT.

reaction with 4-bromoaniline was achieved stereoselectively under palladium catalyzed conditions, then cyclized to give the syn tetrahydroquinoline **65** using sodium borohydride and magnesium chloride.⁴¹ *N*-Acylation of the tetrahydroquinoline was followed by a Suzuki coupling of the 6-bromo group with {4-[(ethoxy)carbonyl]phenyl}boronic acid to give **67**. Deprotection of the 4-aminotetrahydroquinoline was achieved using aluminum chloride and triethylamine to give **68**. The

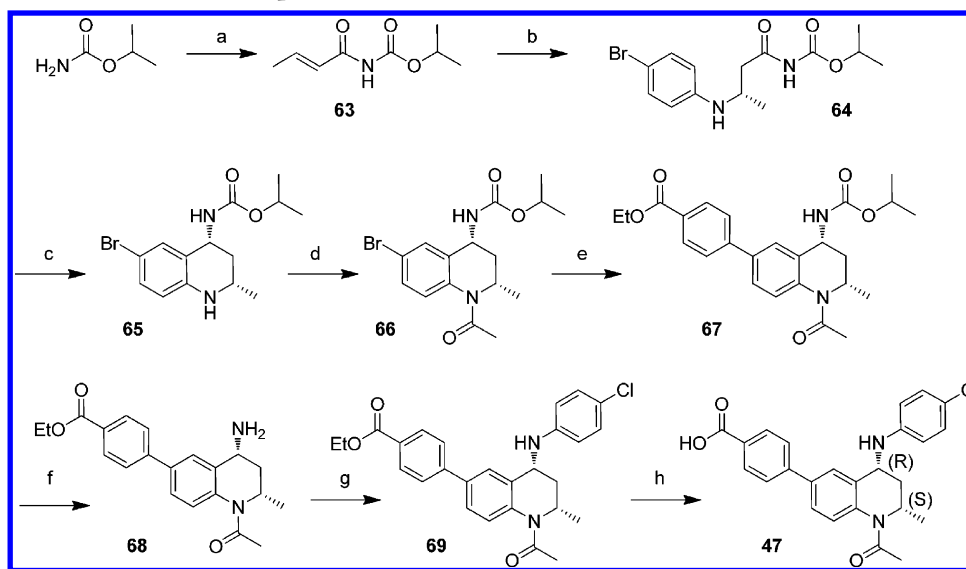
Scheme 5. Synthesis of 2-*H* Tetrahydroquinoline Compound 45^a

^aReagents and conditions: (a) NBS, DCM, 0 °C to RT, 86%; (b) Ac₂O, 80 °C, 69%; (c) 4-MeOPhB(OH)₂, Pd(PPh₃)₄, Cs₂CO₃, DME, H₂O, reflux, 67%; (d) aniline, TiCl₄, TEA, THF/DCM, 0 °C to RT then NaBH(OAc)₃, AcOH, RT, 15%.

mechanism of this deprotection is not fully understood but requires between 3 and 4 equiv of aluminum chloride; typically, we used 3.6 equiv to achieve full conversion. Fewer than 3 equiv of aluminum chloride gave no reaction, while 4 or more equiv of aluminum chloride, by contrast, resulted in the very

Scheme 4. Synthesis of Basic Tetrahydroquinoline Compounds, e.g., 23–26 and 40^a

^aReagents and conditions: (a) 3- or 4-formylPhB(OH)₂, Pd(PPh₃)₄, Na₂CO₃, DME, H₂O, reflux; (b) NaBH(OAc)₃, AcOH, cyclic II^{ary} amines, solvent, RT; (c) MeOH, 6M HCl, reflux; (d) R₄PhB(OH)₂, Cu(OAc)₂, TEA, DCM, RT.

Scheme 6. Enantioselective Route to Compound 47^a

^aReagents and conditions: (a) crotonyl chloride, lithium *tert*-butoxide, THF, $-20\text{ }^{\circ}\text{C}$, 29%; (b) 4-bromoaniline, (R-BINAP)Pd(MeCN)₂(OTf)₂, toluene, THF, $20\text{ }^{\circ}\text{C}$, 67%, ee = 92%; (c) NaBH₄, MgCl₂·6H₂O, EtOH, H₂O, $-15\text{ }^{\circ}\text{C}$, 78%, 1 *cis*-isomer, ee = 92%; (d) AcCl, pyridine, CH₂Cl₂, $0\text{ }^{\circ}\text{C}$, 78%, purification by chiral chromatography, ee >99%; (e) {4-[(ethoxy)carbonyl]phenyl}boronic acid, Pd(PPh₃)₄, NaHCO₃, EtOH, H₂O, $80\text{ }^{\circ}\text{C}$, 92%; (f) AlCl₃, Et₃N, MeOH, CH₂Cl₂, $0\text{ }^{\circ}\text{C}$, 98%; (g) 1-bromo-4-chlorobenzene, DavePhos, Bis(dibenzylideneacetone)palladium, sodium *tert*-butoxide, toluene, $70\text{ }^{\circ}\text{C}$, 37% (94% based on recovered starting material); (h) 2M NaOH, EtOH, RT, 77%.

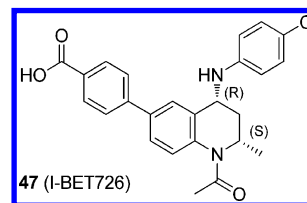
rapid degradation of the starting material to a mixture of unidentified products. The Hartwig–Buchwald reaction with 1-bromo-2-chlorobenzene is sensitive to the quality of the sodium *tert*-butoxide as any acid formed by ester hydrolysis of **68** is unreactive and remains as a byproduct following the reaction. Basic ester hydrolysis completed the synthesis of **47**.

Potency and Selectivity. Knowing that compound **47** is a BET bromodomain inhibitor, we profiled it in additional binding and selectivity assays. Besides having activity in the FA assay, **47** is a potent competitor of labeled histone peptide binding to all four BET isoforms in TR-FRET format, with IC₅₀ at or below 100 nM against each (Table 5). To confirm this, the *K*_d was measured by surface plasmon resonance (SPR) and determined to be 20–25 nM (Supporting Information, Figure S2). Isothermal titration calorimetry (ITC) results suggested that **47** binds to the tandem bromodomain of His-tagged-BRD4 (1–477) with 2:1 stoichiometry, consistent with the binding of one molecule at each bromodomain site, with high affinity (*K*_D 4.4 ± 0.9 nM).³⁷

Compound **47** was tested in a range of fluorescence thermal melting assays (Supporting Information Table S3) and showed no significant interaction with any bromodomain tested other than the BET family and CREBBP. Consistent with this, in a panel of recombinant bromodomain acetyl-lysine site directed binding assays (Table 6, Supporting Information Figure S1), only weak activity was found against other bromodomains apart from CREBBP and EP300. To estimate the true selectivity for BRD4 over CREBBP, isothermal titration calorimetry experiments were carried out, which confirmed that, as expected, **47** binds in a 1:1 ratio with the single bromodomain of CREBBP and that the *K*_d was 6.3 μM, >1000-fold weaker than that for BRD4.³⁷

To assess its selectivity against targets unrelated to bromodomains, **47** was screened in a panel of 50 receptor, ion channel and transporter assays (Supporting Information, Table S4). No significant activity was found at 1 or 10 μM

Table 5. Properties of Compound 47



| | | 47 |
|---|--------|-----------------|
| peptide-based FRET (pIC ₅₀) | BRD2 | 7.4 ± 0.06 (6) |
| | BRD3 | 7.1 ± 0.03 (5) |
| | BRD4 | 7.0 ± 0.20 (39) |
| | BRDT | 7.3 ± 0.25 (4) |
| <i>K</i> _d by SPR (nM) | BRD2 | 25 ± 8 |
| | BRD3 | 20 ± 5 |
| | BRD4 | 23 ± 7 |
| <i>K</i> _d by ITC (nM) ³⁷ | BRD4 | 4.4 ± 0.9 |
| | CREBBP | 6300 ± 500 |
| LPS-stimulated IL6 pIC ₅₀ | PBMC | 7.3 ± 0.25 (20) |
| | HWB | 6.4 ± 0.2 (12) |
| solubility (μg/mL) | FASSIF | 106 |

(<25%), indicating a high degree of selectivity against those classes of nonbromodomain targets included.

Preclinical Developability Profile. Compound **47** showed an improved P450 profile over **28** (Table 7), with low potential to inhibit the major human CYP isoforms (IC₅₀ values >10 μM). In vitro clearances determined with liver hepatocytes were low across all species, including human (CL_i <1.7 mL/min/g liver). Compound **47** had medium permeability in an artificial membrane assay. However, using singly expressed human recombinant enzymes **47** was shown to be a

Table 6. Selectivity of 47^a

| bromodomain | modifier | pIC ₅₀ |
|-----------------------------------|----------|-------------------|
| ATAD2 | < | 4.5 |
| ATAD2B | < | 4.5 |
| BAZ2A | < | 4.5 |
| BAZ2B | < | 4.5 |
| BPTF/FALZ | < | 4.5 |
| BRD1 | < | 4.5 |
| BRD2(1) | | 8.5 |
| BRD2(2) | | 9.2 |
| BRD3(1) | | 8.7 |
| BRD3(2) | | 9.4 |
| BRD4(1) | | 8.5 |
| BRD4(2) | | 9.4 |
| BRD4(1,2) | | 9.6 |
| BRD4 (full-length, short isoform) | | 8.9 |
| BRD1 | < | 4.5 |
| BRD7 | < | 4.5 |
| BRD9 | < | 4.5 |
| BRDT(1) | | 8.4 |
| BRDT(2) | | 9.0 |
| BRPF1 | < | 4.5 |
| BRPF3 | < | 4.5 |
| CECR2 | < | 4.5 |
| CREBBP | | 6.5 |
| EP300 | | 6.2 |
| GCN5 | < | 4.5 |
| PBRM1(2) | | 5.1 |
| PBRM1(5) | < | 4.5 |
| PCAF | < | 4.5 |
| SMARCA2 | < | 4.5 |
| TAF1(2) | | 5.0 |
| TAF1L(2) | | 4.8 |
| TIF1 α /TRIM24 (BD) | | 5.0 |
| TIF1 α /TRIM24 (PHD + BD) | | 4.8 |
| TIF1 γ /TRIM33 (PHD + BD) | < | 4.5 |
| WDR9(2) | | 4.7 |

^aActivity in BROMOscanSM recombinant protein binding assays carried out at DiscoverRx (<http://www.discoverx.com>).

time-dependent inhibitor of CYP3A4 based on a 4-fold shift in IC₅₀. Its free fraction was also relatively low.

The pharmacokinetic properties of compound 47 were investigated in four preclinical species: mouse, rat, dog, and nonhuman primate (Table 8). It had a low-moderate clearance across the preclinical species (<30% liver blood flow). Consistent with this, 47 was stable in vitro in hepatocytes from preclinical species. The in vitro/in vivo clearance correlation across preclinical species indicates that, based on human in vitro clearance, human blood clearance could be low to moderate. The volume of distribution was low to moderate (0.5–1.0 L/kg), indicating some distribution into the tissues. Elimination half-life was moderate in dog and primate (1.8 and 2.7 h, respectively) and longer in mouse (3.6 h). Compound 47 therefore has the potential to be administered once or twice daily in human. Oral bioavailability was moderate in the rat (ca. 28%) and higher in mouse, dog, and primate (90%, 80%, and 100%, respectively). The systemic exposure in mouse was suitable for exploration of the pharmacodynamics in vivo, and exposures achieved in the rat and dog via the oral route allow for progression to safety assessment evaluation in these species.

Table 7. Properties of Compound 47

| | | 47 |
|---|----------------------|---|
| hepatocyte clearance (mL/min/g tissue) | mouse | <0.85 |
| | rat | <0.85 |
| | dog | <1.7 |
| | primate ^a | <0.85 |
| | human | <0.85 |
| P450 profile IC ₅₀ (μ M) ^b | 1A2 (ER) | >33 |
| | 2C9 (FCA) | 13 |
| | 2C19 (BMC) | 12 |
| | 2D6 (MMMC) | >33 |
| | 3A4 (7BQ) | 32 |
| | 3A4 (DEF) | 21 |
| time-dependent P450 inhibition | 3A4 (DEF) | 4-fold shift in IC ₅₀ over 30 min (>100 μ M to 24 μ M) |
| permeability (nm/s) | artificial membrane | 95 |
| free fraction (F_{ub}) ^c | mouse | 0.013 |
| | rat | 0.009 |
| | dog | 0.065 |
| | human | 0.017 |

^aCynomolgus monkey. ^bFluorometric assay with Cypex cDNA expressed isoforms. ^cMeasured using rapid equilibrium dialysis at a nominal concentration of 1000 ng/mL. Assay performed using blood.

Oral Activity. We have previously reported the activity of compound 47 in neuroblastoma assays.³⁷ Because of the links between ApoA1 up-regulation, BET inhibition, and inflammatory disease that emerged as this work was underway,⁷ compound 47 was assessed in an acute mouse inflammation model. After a single oral administration of compound at various concentrations followed by intraperitoneal LPS challenge, the effect on hepatic mRNA expression of the acute phase protein PAI-1 was measured. The compound showed dose-dependent inhibition of PAI-1 expression, with very significant activity already observed at the 3 mg/kg dose (Figure 2).

Intravenous Activity in a Mouse Septic Shock Model.

Sepsis is an acute inflammatory condition characterized by high mortality rates and a significant unmet medical need despite considerable research effort.³⁸ Therefore, compound 47 was tested in a mouse septic shock model using a therapeutic mode of treatment (dosing after induction of sepsis). An intraperitoneal injection of LPS (15–20 mg/kg) was first administered to Balb/c mice. When clinical signs were observed, compound 47 was intravenously dosed at 10 mg/kg. Only 25% of mice in the vehicle group survived, while 56% of mice treated with compound survived after 5 days (Figure 3), indicating that compound 47 is able to prevent death of diseased animals following a single administration.

Binding Modes of Optimized Tetrahydroquinolines.

In a previous publication, we showed the structure of the racemic tetrahydroquinoline 48 (Figure 4A) as an example of a fragment binding to the N-terminal bromodomain of BRD2.²⁹ The amino acids of the BET family of bromodomains are highly conserved in the acetyl-lysine pocket (Figure 4B), so it is not surprising that 47 in BRD4 inherits the general binding

Table 8. Preclinical Pharmacokinetic Parameters for Compound 47 (Values are Mean $n = 3$, IV Infusion at 1 mg/kg, and PO Dose at 3 mg/kg unless Otherwise Stated)

| species | CLb (mL/min/kg) | V_{ss} (L/kg) | $t_{1/2}$ iv (h) | AUC _{0-t} po (ng·h/mL) | F_{po} (%) |
|----------------------|-----------------|-----------------|------------------|---------------------------------|--------------|
| mouse ^a | 3.1 ± 0.4 | 0.48 ± 0.1 | 3.6 ± 0.2 | 6028 | 45 |
| rat ^b | 26 ± 4 | 2.0 ± 0.4 | >8 | 539 ± 96 | 28 ± 1 |
| beagle dog | 6.0 ± 1 | 0.8 ± 0.1 | 1.8 ± 0.6 | 5900 ± 968 | 80 ± 12 |
| primate ^c | 3.0 ± 0.9 | 1.0 ± 0.4 | 2.7 ± 0.1 | 10968 ± 3852 | 103 ± 35 |

^aBalb/c bolus IV dose at 10 mg/kg. ^bTerminal $t_{1/2}$ estimated from $n = 1$ rat. ^cCynomolgus monkey, IV infusion at 1 mg/kg, and PO dose at 2 mg/kg. Parameters are from plasma analysis.

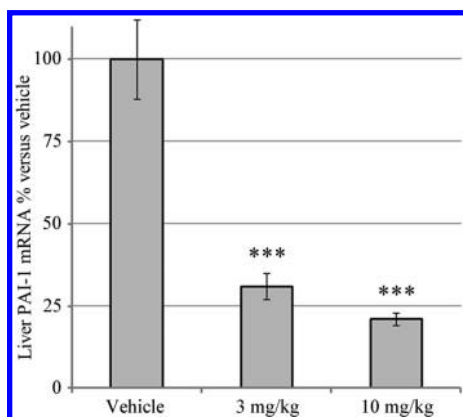


Figure 2. Oral activity of 47 in a murine acute LPS challenge model: PAI-1 mRNA relative to vehicle (mean ± SEM, $n = 8$). (***) p value <0.0001 following a t test comparison to the vehicle-treated group.

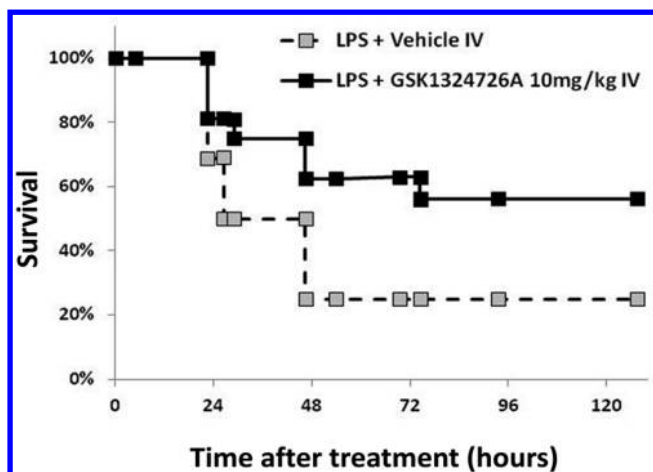


Figure 3. Intravenous activity of 47 in a murine septic shock model (mean of two independent experiments with $n = 8$ per group in each study).

mode of fragment 48 in BRD2 (Figure 5A). This includes the key directional interactions between the THQ scaffold and the acetyl-lysine site of BRD4, namely the hydrogen bond between the N1-acetyl group and the side chain NH_2 of the conserved asparagine Asn140. The N1-acetyl group forms a second, shorter hydrogen bond to a water molecule, which itself hydrogen bonds to the side chain hydroxyl of Tyr97. Our analysis of fragment complexes with BRD2 suggested that the water interaction may be the stronger of the two. This water molecule is one of a chain of four conserved within bromodomain crystal structures published to date. Lying at the bottom of the acetyl-lysine pocket, these form a highly satisfied H-bonding network connecting Tyr97 to the backbone carbonyls of Pro82 and Gln85. The H-bonding interactions of

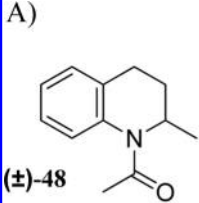
the THQ template mimic the interactions made by the acetyl-lysine side chain found in X-ray structures of the BET bromodomains bound to acetylated peptides (Figure 5B).^{29,39} The methyl group of the N1-acetyl of the THQ fills the small pocket between the buried water chain and the aromatic side chain of Phe83 in the same position as the terminal methyl of the acetyl lysine side chain.

The crystal structure of the racemic fragment 48 in BRD2 showed that the bound enantiomer had (*S*) absolute chirality at the C2 position and that the 2-methyl group filled a small lipophilic pocket near Leu110 in the ZA loop. The C2 methyl group of 47 fulfils the same role and makes direct contact with the analogous BRD4 residue Leu94 (Figure 5C). The vector projecting from the C2 hydrogen points toward the side chain carbonyl oxygen of Asn140, which is only 3.5 Å away (Figure 5A). Even a substituent as small as a methyl group would clash with this carbonyl oxygen, explaining the (2*S*) stereochemical requirement for activity.

The unsaturated ring of the THQ is sandwiched by hydrophobic residues (mainly Pro82 and Leu92) in a narrow lipophilic region at the base of the ZA channel (Figure 5C). The 6-substituent phenyl ring extends further through this channel toward solvent, passing close by Trp81 in an edge-to-face arrangement. This location explains the gross SAR seen at the 6-position in the BET binding assays. The presence of the 6-aryl ring in compounds such as 16 increases BET potency compared to analogues like 12 because of lipophilic interactions with the channel, particularly with Trp81. The crystal structure also shows that the meta and especially the para positions of the 6-aryl ring point away from the protein surface, explaining the wide range of tolerated substitutions including acidic and basic groups in compounds 17–25. The carboxylate of 47 makes no direct interaction with the protein but does lie in the rough vicinity of the side chain of Lys91, although because of its flexibility this probably does not contribute much to the binding free energy. The ortho position of the 6-aryl ring offers greater opportunities for interaction with the protein. One ortho position lies close to the BRD4 WPF motif (Trp81–Pro82–Phe83), with limited room for growth (Figure 5B). The opposite ortho position has more accessible space, but the SAR shows that substitution is detrimental to binding (compound 44). This can be understood by considering the torsion angle between the THQ core and the 6-phenyl ring, which is about 30°. Ortho groups would increase this torsion angle and the width of the ligand within the ZA channel, leading to closer steric contacts against Trp81 and Leu92.

The THQ 4-position anilino linker adopts near optimal torsional angles for this group and directs its substituent chlorophenyl ring toward the hydrophobic “WPF shelf” (named because of its proximity to the conserved bromodomain WPF motif defined above). This lipophilic site has been shown to be important in other classes of BET inhibitor,^{30,31,33}

A)



B)

| BRD2 N | BRD2 C | BRD3 N | BRD3 C | BRD4 N | BRD4 C | BRD4 N | BRD4 C | BRDT N | BRDT C | BET consensus | CREBBP | Location |
|-----------|-----------|-----------|-----------|-----------|-----------|-----------|-----------|-----------|-----------|------------------|--------|-------------------|
| W97 | W370 | W57 | W332 | W81 | W374 | W50 | W293 | | | Trp | L1109 | WPF motif* |
| P98 | P371 | P58 | P333 | P82 | P375 | P51 | P294 | | | Pro | P1110 | WPF motif* |
| F99 | F372 | F59 | F334 | F83 | F376 | F52 | F295 | | | Phe | F1111 | WPF motif* |
| Q101 | K374 | Q61 | K336 | Q85 | K378 | R54 | N297 | | | POLAR | Q1113 | ZA channel* |
| P102 | P375 | P62 | P337 | P86 | P379 | P55 | P298 | | | Pro | P1114 | ZA channel |
| V103 | V376 | V63 | V338 | V87 | V380 | V56 | V299 | | | Val | V1115 | ZA channel* |
| D104 | D377 | D64 | D339 | D88 | D381 | D57 | D300 | | | Asp | D1116 | ZA loop |
| L108 | L381 | L68 | L343 | L92 | L385 | L61 | L304 | | | Leu | L1120 | ZA loop* |
| L110 | L383 | L70 | L345 | L94 | L387 | L63 | L306 | | | Leu | I1122 | ZA loop* |
| Y113 | Y386 | Y73 | Y348 | Y97 | Y390 | Y66 | Y309 | | | Tyr | Y1125 | Water-binding Tyr |
| M148 | M421 | M108 | M383 | M132 | M425 | M101 | M344 | | | Met | M1160 | B-helix |
| N151 | N424 | N111 | N386 | N135 | N428 | N104 | N347 | | | Asn | N1163 | B-helix |
| C152 | C425 | C112 | C387 | C136 | C429 | C105 | C348 | | | Cys | A1164 | B-helix* |
| Y155 | Y428 | Y115 | Y390 | Y139 | Y432 | Y108 | Y351 | | | Tyr | Y1167 | Conserved Tyr* |
| N156 | N429 | N116 | N391 | N140 | N433 | N109 | N352 | | | Asn | N1168 | Conserved Asn* |
| D160 | H433 | D120 | H395 | D144 | H437 | D113 | H356 | | | POLAR | S1172 | |
| D161 | D434 | D121 | E396 | D145 | E438 | D114 | E357 | | | NEGATIVE | R1173 | WPF shelf* |
| I162 | V435 | I122 | V397 | I146 | V439 | I115 | V358 | | | ALIPHATIC | V1174 | Gatekeeper* |
| M165 | M438 | M125 | M400 | M149 | M442 | M118 | M361 | | | Met | F1177 | WPF shelf* |

Figure 4. (A) Tetrahydroquinoline fragment 48. (B) Conservation of the BET family and CREBBP bromodomain acetyl-lysine sites. Colors represent residue properties: green = hydrophobic, red = acidic, blue = basic, orange = polar, purple = proline, white = small. * denotes residue is in contact (≤ 4.5 Å) with compound 47 in BRD4 N-terminal bromodomain crystal structure (PDB 3uvw).³⁹

and the poor activity of **26** and **27** which lack this substituent supports its importance in the THQ series. One edge of the chlorophenyl ring makes direct hydrophobic contacts with the WPF shelf (the 2-position with Ile146, and the 3-position with Trp81 and Pro82) but the opposite face points toward solvent (Figure 5C). There is therefore plenty of space for ortho or meta substituents on this ring, explaining the rather flat substituent effects on activity at these positions. The 4-chloro group lies near Trp81 and contacts the hydrophobic side chain of Met149, although this is near the outside of the shelf and exposed to solvent, so this might make relatively small contributions to activity. Because all of the interactions made by the 4-anilino chlorophenyl ring are hydrophobic, they are not very directional, and modifications to the ring may be accommodated by relatively small sliding movements over the WPF shelf surface, as found previously in a dimethyl isoxazole series.³¹

Comparison of Binding Mode to Selected Literature BET Inhibitors. Figure 6A shows the BRD4 N-terminal bromodomain binding mode of THQ **47** superimposed on that of compound **1**.⁴ These different chemotypes overlay very closely, with the N1 acetyl group of **47** fulfilling a similar role to the triazole ring of **1** in its interaction with Asn140 and the conserved water network. The polycyclic cores of both inhibitors also overlay very closely, as do the chlorophenyl rings of each, which approach the WPF shelf from the same direction and make similar interactions (Figure 6A). Compound **3** binds in a very different manner, both in chemical structure and also in the directionality of the approach of its aryl ring to the WPF shelf (Figure 6B).²⁵

Binding Mode in other BET Bromodomains. X-ray structures of **47** were also solved in complex with the N-terminal and C-terminal bromodomains of BRD2 (Figure 7A,B). Both binding modes are very similar to that seen in the

N-terminal bromodomain of BRD4. This is as expected, given the conservation of residues involved in direct interactions with the inhibitor (Figure 4B). The only differences are relatively small movements of the 4-anilino chlorophenyl group. Because of the nonpolar, weakly directional nature of the interactions between the chlorophenyl and the WPF shelf, these small movements do not translate into significant differences in potency between the BET isoforms (Table 5).

An X-ray structure of the N-terminal bromodomain of BRD2 was also solved in complex with **28**. The majority of the structure is well resolved in chains A and B, although the ligand is not visible in chain C. Compound **28** adopts a very similar binding mode to that of **47** (Figure 7C), but the electron density for the methylpiperidine is weak (Supporting Information Figure S3) and in neither chain does this group make apparent strong interactions. This is consistent with the small effect of this substituent on binding affinity (e.g., **28** relative to **19**).

CONCLUSION

The discovery and optimization of the tetrahydroquinoline series which led to **47** was accomplished without the benefit of any knowledge of the molecular target. Its molecular mechanism is now well understood. This series joins a growing list of different chemotypes which produce potent biological effects by binding to the BET family of bromodomains. We have recently shown that **47** is a potent suppressor of MYCN expression and survival in neuroblastoma cell lines and xenograft growth.³⁷ Here, we have described its discovery and potent anti-inflammatory effects. The THQ series offers chemical tractability and an attractive range of properties suitable for optimization and progression to preclinical development. Further publications will describe more of the

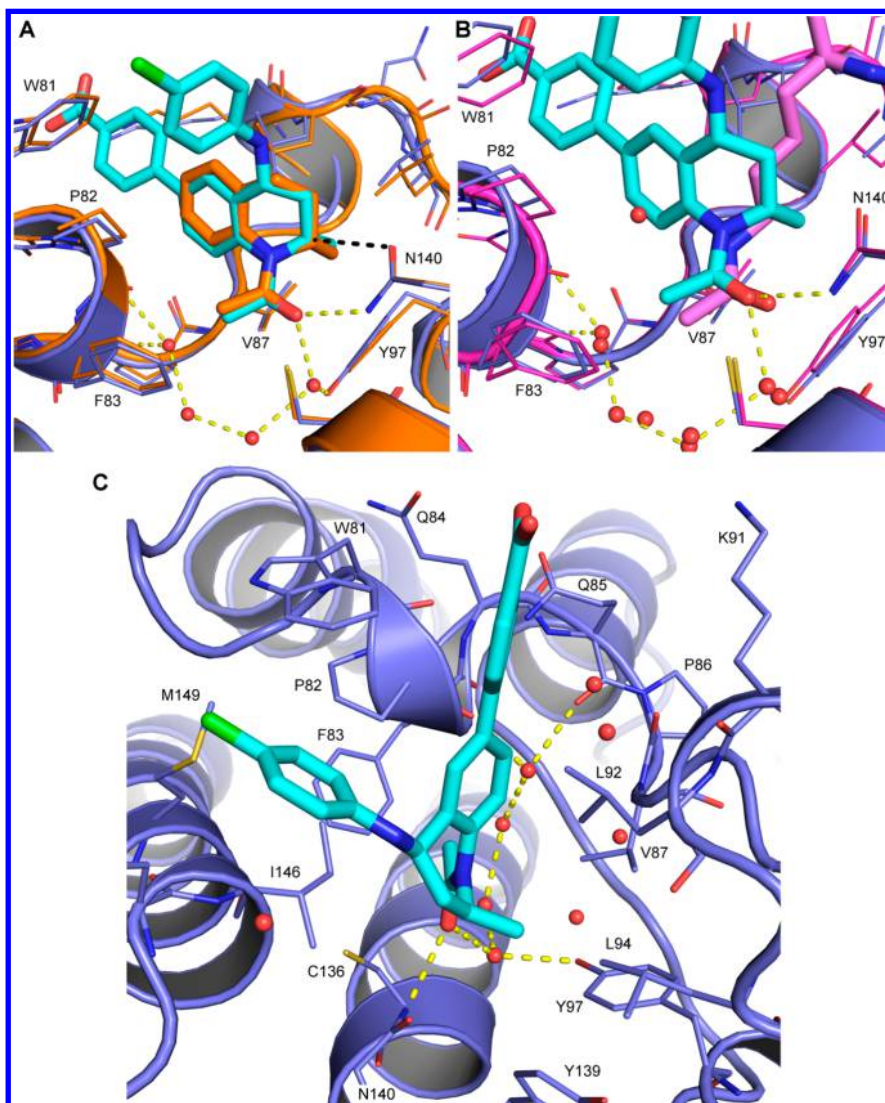


Figure 5. Crystal structure of 47 (cyan carbons) in the BRD4 N-terminal bromodomain (blue carbons). The conserved H-bonding network between inhibitor, protein, and conserved waters is marked in yellow. (A) Comparison with X-ray structure of fragment 48 in BRD2 N-terminal domain (orange). Black dotted line indicates the 3.5 Å distance between the C2 carbon of 47 and the side chain oxygen of Asn140. (B) Comparison to acetyl-lysine (purple carbons) taken from X-ray structure of histone H4(1-12)K5AcK8Ac in BRD4 (PDB 3uvv).³⁹ (C) Key hydrogen-bonding interactions of 47 with BRD4.

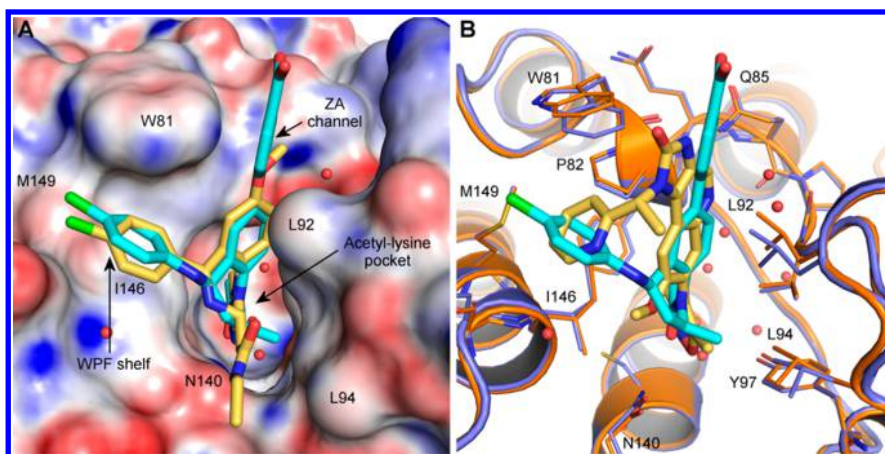


Figure 6. (A) THQ 47 (cyan carbons) bound to BRD4 N-terminal bromodomain, with BRD4 molecular surface generated with modeled hydrogen atoms, aligned to 1 (yellow, PDB 3p5o). (B) Binding mode of 47 in BRD4 N-terminal bromodomain compared to that of 3 (yellow, PDB 3zyu).

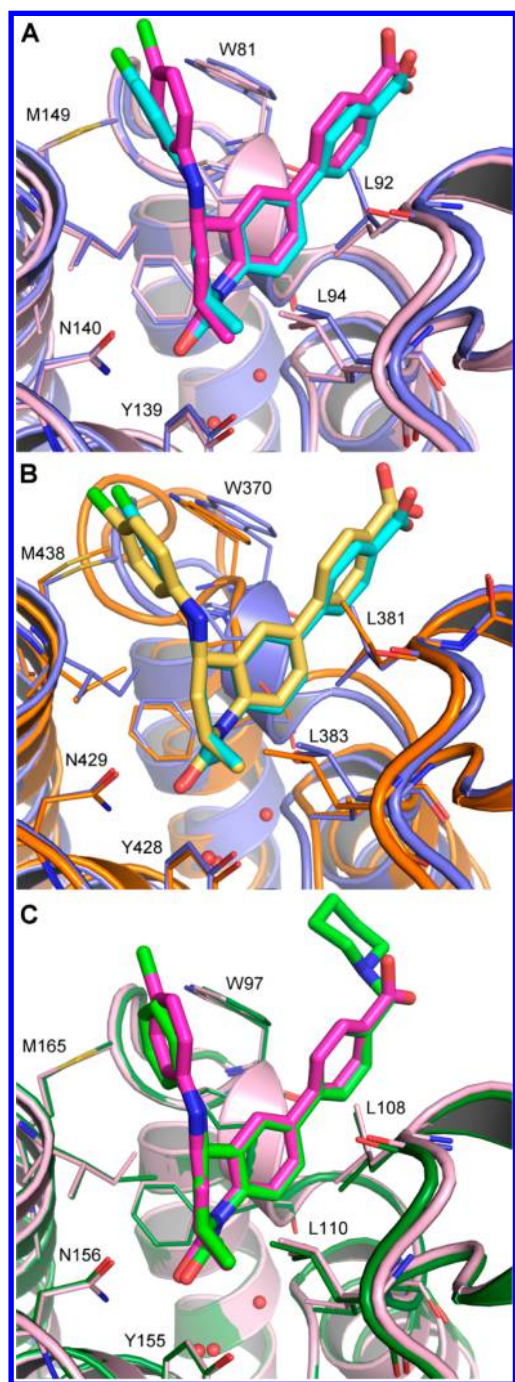


Figure 7. Comparison between X-ray structures of **47** in complex with BRD4 N-terminal bromodomain (cyan/blue) and (A) BRD2 N-terminal bromodomain (pink/purple), with BRD4 residue numbering, and (B) BRD2 C-terminal bromodomain (yellow/orange), with BRD2 residue numbering. (C) Comparison of X-ray structures of BRD2 N-terminal bromodomain in complex with **47** (pink/purple) and with **28** (chain A, green), with BRD2 N-terminal numbering.

medicinal chemistry and biology around this template targeting a range of therapeutic areas.

EXPERIMENTAL SECTION

General Experimental Methods (Chemistry). All solvents were purchased from Sigma-Aldrich (Hy-Dry anhydrous solvents) and commercially available reagents were used as received. Melting points were recorded on Buchi B-545 apparatus and are uncorrected. All

reactions were followed by TLC analysis (TLC plates GF254, Merck) or liquid chromatography mass spectrometry (LCMS) using a Waters ZQ instrument. NMR spectra were recorded on a Bruker NanoBay 400 MHz or a Bruker AV++ 600 MHz spectrometer and are referenced as follows. ^1H NMR (400 or 600 MHz), internal standard TMS at $\delta = 0.00$. ^{13}C NMR (100.6 or 150.9 MHz), internal standard CDCl_3 at $\delta = 77.23$ or $\text{DMSO}-d_6$ at $\delta = 39.70$. Column chromatography was performed on prepacked silica gel columns (30–90 mesh, IST) using a Biotage SP4. Mass spectra were recorded on Waters ZQ (ESI-MS) and Q-ToF 2 (HRMS) spectrometers. Mass directed auto prep was performed on a Waters 2767 with a MicroMass ZQ mass spectrometer using Supelco LCABZ++ column. Reactions performed under microwave irradiation utilized either a Biotage Initiator or CEM Discover Microwave.

Abbreviations for multiplicities observed in NMR spectra: s; singlet; br s, broad singlet; d, doublet; t, triplet; q, quadruplet; p, pentuplet; spt, septuplet; m, multiplet. The purity of all compounds was determined by LCMS and ^1H NMR and was always >95%. For detailed LCMS/MDAP methodology see Supplementary Methods, Supporting Information.

General Procedure for the Formamide Deprotection (Method A). To a suspension of formamide (1 equiv) in MeOH (0.3 mol/L) was added 6 N HCl (3 equiv). The resulting mixture was stirred at reflux for 3 h, and the medium was made basic by the addition of 2N NaOH. The MeOH was evaporated under reduced pressure and the organic material extracted with EtOAc. The organic layer was washed with brine, dried over Na_2SO_4 , and concentrated to dryness to afford the desired primary amine.

General Procedure for the Chan–Lam Coupling (Method B). A mixture of the amine (1 equiv), phenyl boronic acid (3 equiv), anhydrous copper acetate (1.5 equiv), and triethylamine (3 equiv) in dry DCM (0.3 mol/L) was stirred at room temperature for 48–72 h. Progression of the reaction was monitored by TLC, and if necessary an additional equivalent of phenyl boronic acid and triethylamine was added and the mixture allowed to stir at room temperature for a further 12 h. This operation was repeated until the amount of the expected product exceeded the remaining proportion of the starting intermediate. The resulting mixture was poured into water, and the organic phase was extracted with DCM, dried over Na_2SO_4 , filtered, and evaporated to dryness. The residue was purified by recrystallization or chromatography on silica gel.

General Procedure for the Suzuki Coupling (Method C). To a solution of bromo derivative (100 mg, 0.28 mmol) in 1,2-dimethoxyethane (0.1 mol/L) was added boronic acid or the corresponding boronate ester (1.5 equiv), a 2N solution sodium carbonate in water (5 equiv), and $\text{Pd}(\text{PPh}_3)_4$ (0.05 equiv), and the mixture was stirred under reflux for 20 h. The solvent was then removed under reduced pressure, and EtOAc was added to the residue. The organic phase was washed with brine, dried over Na_2SO_4 , filtered, and evaporated to dryness. The residue was purified by recrystallization or chromatography on silica gel.

General Procedure for Ester Hydrolysis (Method D). A solution of ester (1 equiv) in EtOH (0.1 mol/L) and 1N NaOH (2 equiv) was heated to 60 °C. After 1 h, the mixture was evaporated to dryness and the residue taken up in water. Acetic acid was added until pH 4–5, and the aqueous layer was extracted with DCM (2X). The combined organic layers were washed with brine and dried over Na_2SO_4 . After concentration under reduced pressure, the title compound was obtained as a solid.

General Procedure for Reductive Amination (Method E). To a solution of aldehyde (1 equiv) and piperidine (1.2 equiv) in solution in dichloroethane (0.1 mol/L) were added at room temperature triacetoxysodiumborohydride (1.3 equiv) and acetic acid (2.2 equiv). After stirring 2 h, the mixture was poured into a saturated aqueous solution of NaHCO_3 . The organic layer was extracted with DCM and washed with brine, dried over Na_2SO_4 , filtered, and evaporated to dryness. The residue was purified by recrystallization or chromatography on silica gel.

cis-1-(2-Methyl-4-(p-tolylamino)-3,4-dihydroquinolin-1(2H-yl)ethanone (10) and trans-1-(2-Methyl-4-(p-tolylamino)-3,4-

dihydroquinolin-1(2H)-yl)ethanone (11). To a solution of 1-acetyl-2-methyl-2,3-dihydroquinolin-4(1H)-one (**51**) (1 g, 4.9 mmol), 4-methylaniline (0.63 g, 5.9 mmol) and TEA (3.0 mL, 21.2 mmol) in THF (50 mL) at 0 °C was added TiCl₄ (1 M in CH₂Cl₂, 7.4 mL, 7.4 mmol). The reaction mixture was stirred for 2 h at room temperature, and TiCl₄ (1 M in CH₂Cl₂, 4.9 mL, 4.90 mmol) was added again. After 3 more hours, sodium borohydride (1.49 g, 39.36 mmol) was added portion by portion at room temperature. The reaction mixture was stirred for 18 h then poured into a 2 M aqueous solution of NaHCO₃. The organic layer was extracted with CH₂Cl₂ and washed with brine, dried over Na₂SO₄, filtered, and evaporated to dryness to afford a mixture of two isomers *cis/trans*. The residue was purified by chromatography on silica gel (5% MeOH in CH₂Cl₂) to provide the two isomers. Compound **10**: isolated as an orange oil (65 mg, 4.5%). ¹H NMR (300 MHz, CDCl₃) δ ppm 7.30 (m, 1H), 7.21 (m, 1H), 7.10 (m, 2H), 6.90 (m, 1H), 6.55 (m, 1H), 4.82 (m, 1H), 4.51 (m, 1H), 2.50 (m, 1H), 2.19 (m, 1H), 2.16 (s, 3H), 2.09 (s, 3H), 1.69 (m, 2H), 1.13 (m, 1H), 1.10 (d, J = 6.6 Hz, 3H). Compound **11**: isolated as an orange oil (130 mg, 9%). ¹H NMR (300 MHz, CDCl₃) δ ppm 7.25 (m, 2H), 7.11 (m, 2H), 6.92 (m, 2H), 6.48 (m, 2H), 4.82 (m, 1H), 4.14 (m, 1H), 3.63 (m, 1H), 2.56 (m, 1H), 2.18 (s, 3H), 2.11 (s, 3H), 1.19 (m, 1H), 1.07 (d, J = 6.4 Hz, 3H). LCMS (method formate, 5 min): retention time 2.07 min, [M + H]⁺ = 294.0. HRMS (M + H)⁺ 294.18.

1-((2S*,4R*)-2-Methyl-4-(phenylamino)-3,4-dihydroquinolin-1(2H)-yl)ethanone (12). To a solution of 1-acetyl-2-methyl-2,3-dihydroquinolin-4(1H)-one (**51**) (4.06 g, 20 mmol) and aniline (3.65 mL, 40 mmol) in CH₂Cl₂ (300 mL) at 0 °C was added TiCl₄ (1 M in CH₂Cl₂, 30 mL, 30 mmol) over 30 min. The reaction mixture was allowed to warm to room temperature and stirred for 16 h. NaBH₄ (6.1 g, 160 mmol) was then added portion by portion at room temperature. The resulting mixture was stirred for 4 h and then was treated with a 10% w/w Na₂CO₃ aqueous solution. The layers were separated, and the organic phase was extracted with CH₂Cl₂. The combined organic phases were dried over Na₂SO₄, filtered, and evaporated to dryness to afford a mixture of two isomers *cis/trans*. The residue was purified by chromatography on silica gel (5% MeOH in CH₂Cl₂) to give **12** (3.2 g, 57%) as an orange oil. LCMS (method formate): retention time 1.09 min, [M + H]⁺ = 281.24. ¹H NMR (400 MHz, DMSO-*d*₆) δ 7.22–7.33 (m, 2H), 7.16 (m, 2H), 7.09 (m, 2H), 6.65 (d, J = 7.6 Hz, 2H), 6.56 (t, J = 7.3 Hz, 1H), 6.02 (d, J = 7.8 Hz, 1H), 4.71 (m, 1H), 4.18 (m, 1H), 2.59 (m, 1H), 2.08 (s, 3H), 1.19 (m, 1H), 1.4 (d, J = 6.4 Hz, 3H).

1-((2S*,4R*)-2-Methyl-6-phenyl-4-(phenylamino)-3,4-dihydroquinolin-1(2H)-yl)ethanone (16). Method C was used starting from 1-((2S*,4R*)-6-bromo-2-methyl-4-(phenylamino)-3,4-dihydroquinolin-1(2H)-yl)ethanone (**56**) and phenylboronic acid; mp 186 °C. LCMS (method formate): retention time 1.28 min, [M + H]⁺ = 357.28. ¹H NMR (400 MHz, DMSO-*d*₆) δ 7.48–7.58 (m, 3H), 7.38–7.47 (m, 4H), 7.28–7.35 (m, 1H), 7.10 (m, 2H), 6.73 (d, J = 7.8 Hz, 2H), 6.58 (t, J = 7.3 Hz, 1H), 6.06 (d, J = 7.8 Hz, 1H), 4.73 (m, 1H), 4.28 (m, 1H), 2.63 (m, 1H), 2.10 (s, 3H), 1.24 (m, 1H), 1.10 (d, J = 6.4 Hz, 3H).

4-((2S*,4R*)-1-Acetyl-2-methyl-4-(phenylamino)-1,2,3,4-tetrahydroquinolin-6-yl)benzoxonitrile (17). Method C was used starting from 1-((2S*,4R*)-6-bromo-2-methyl-4-(phenylamino)-3,4-dihydroquinolin-1(2H)-yl)ethanone (**56**) and (4-cyanophenyl)boronic acid; mp 104 °C. LCMS (method formate): retention time 1.19 min, [M + H]⁺ = 382.26. ¹H NMR (400 MHz, DMSO-*d*₆) δ 7.89 (d, J = 8.3 Hz, 2H), 7.73 (d, J = 8.3 Hz, 2H), 7.61–7.69 (m, 1H), 7.44–7.55 (m, 2H), 7.11 (d, J = 7.7, 7.8 Hz, 2H), 6.73 (d, J = 7.8 Hz, 2H), 6.55 (t, J = 7.8 Hz, 1H), 6.05 (d, J = 7.8 Hz, 1H), 4.70 (m, 1H), 4.31 (m, 1H), 2.63 (m, 1H), 2.15 (s, 3H), 1.24 (m, 1H), 1.10 (d, J = 6.4 Hz, 3H).

Methyl 4-((2S*,4R*)-1-Acetyl-2-methyl-4-(phenylamino)-1,2,3,4-tetrahydroquinolin-6-yl)benzoate (18). Method C was used starting from 1-((2S*,4R*)-6-bromo-2-methyl-4-(phenylamino)-3,4-dihydroquinolin-1(2H)-yl)ethanone (**56**) and (4-(methoxycarbonyl)phenyl)boronic acid; mp 90 °C. LCMS (method formate): retention time 1.24 min, [M + H]⁺ = 415.32. ¹H NMR (400

MHz, DMSO-*d*₆) δ 8.00 (d, J = 8.3 Hz, 2H), 7.71 (d, J = 8.3 Hz, 2H), 7.63 (d, J = 2.2 Hz, 1H), 7.54 (d, J = 1.5 Hz, 1H), 7.46 (d, J = 8.1 Hz, 1H), 7.12 (m, 2H), 6.74 (d, J = 7.6 Hz, 2H), 6.59 (t, J = 7.8 Hz, 1H), 6.05 (d, J = 8.1 Hz, 1H), 4.67–4.79 (m, 1H), 4.26–4.36 (m, 1H), 3.86 (s, 3H), 2.58–2.71 (m, 1H), 2.08 (s, 3H), 1.18–1.31 (m, 1H), 1.10 (d, J = 6.4 Hz, 3H).

4-((2S*,4R*)-1-Acetyl-2-methyl-4-(phenylamino)-1,2,3,4-tetrahydroquinolin-6-yl)benzoic acid (19). Method D was used to hydrolyze methyl 4-((2S*,4R*)-1-acetyl-2-methyl-4-(phenylamino)-1,2,3,4-tetrahydroquinolin-6-yl)benzoate (**18**); mp 246 °C. LCMS (method formate): retention time 0.70 min, [M – H][–] = 399.38. ¹H NMR (400 MHz, DMSO-*d*₆) δ 12.20–13.44 (br s, 1H), 7.97 (d, J = 8.3 Hz, 2H), 7.59–7.67 (m, 3H), 7.52 (d, J = 1.5 Hz, 1H), 7.45 (d, J = 8.3 Hz, 1H), 7.11 (dd, J = 7.4, 8.4 Hz, 2H), 6.74 (d, J = 8.4 Hz, 2H), 6.59 (t, J = 7.4 Hz, 1H), 6.05 (d, J = 8.1 Hz, 1H), 4.73 (m, 1H), 4.31 (m, 1H), 2.63 (m, 1H), 2.15 (s, 3H), 1.24 (m, 1H), 1.10 (d, J = 6.4 Hz, 3H).

1-((2S*,4R*)-2-Methyl-4-(phenylamino)-6-(4-(trifluoromethyl)phenyl)-3,4-dihydroquinolin-1(2H)-yl)ethanone (20). Method C was used starting from 1-((2S*,4R*)-6-bromo-2-methyl-4-(phenylamino)-3,4-dihydroquinolin-1(2H)-yl)ethanone (**56**) and (4-(trifluoromethyl)phenyl)boronic acid; mp 85 °C. LCMS (method formate): retention time 1.36 min, [M + H]⁺ = 425.18. ¹H NMR (400 MHz, DMSO-*d*₆) δ 7.77 (m, 4H), 7.63 (dd, J = 2.1, 8.2 Hz, 1H), 7.51 (d, J = 1.2 Hz, 1H), 7.48 (d, J = 8.1 Hz, 1H), 7.11 (dd, J = 7.8, 7.8 Hz, 2H), 6.73 (d, J = 7.8 Hz, 2H), 6.58 (t, J = 7.3 Hz, 1H), 6.06 (d, J = 7.8 Hz, 1H), 4.72 (m, 1H), 4.31 (m, 1H), 2.64 (m, 1H), 2.16 (s, 3H), 1.25 (m, 1H), 1.11 (d, J = 6.4 Hz, 3H).

1-((2S*,4R*)-6-(4-Methoxyphenyl)-2-methyl-4-(phenylamino)-3,4-dihydroquinolin-1(2H)-yl)ethanone (21). Method C was used starting from 1-((2S*,4R*)-6-bromo-2-methyl-4-(phenylamino)-3,4-dihydroquinolin-1(2H)-yl)ethanone (**56**) and (4-methoxyphenyl)boronic acid; mp 86 °C (becomes gummy). LCMS (method formate): retention time 1.24 min, [M + H]⁺ = 387.18. ¹H NMR (400 MHz, DMSO-*d*₆) δ 7.42–7.52 (m, 3H), 7.33–7.41 (m, 2H), 7.10 (d, J = 7.7, 7.7 Hz, 2H), 6.98 (d, J = 8.8 Hz, 2H), 6.72 (d, J = 7.8 Hz, 2H), 6.58 (t, J = 7.2 Hz, 1H), 6.05 (d, J = 8.1 Hz, 1H), 4.72 (m, 1H), 4.26 (m, 1H), 3.76 (s, 3H), 2.61 (m, 1H), 2.13 (s, 3H), 1.25 (m, 1H), 1.09 (d, J = 6.4 Hz, 3H).

1-((2S*,4R*)-6-(4-(Hydroxymethyl)phenyl)-2-methyl-4-(phenylamino)-3,4-dihydroquinolin-1(2H)-yl)ethanone (22). Method C was used starting from 1-((2S*,4R*)-6-bromo-2-methyl-4-(phenylamino)-3,4-dihydroquinolin-1(2H)-yl)ethanone (**56**) and (4-(hydroxymethyl)phenyl)boronic acid; mp 102 °C. LCMS (method formate): retention time 1.02 min, [M + H]⁺ = 387.3. ¹H NMR (400 MHz, DMSO-*d*₆) δ 7.54 (dd, J = 2.0, 8.3 Hz, 1H), 7.43–7.5 (m, 3H), 7.32–7.43 (m, 3H), 7.10 (dd, J = 7.8, 7.8 Hz, 2H), 6.73 (d, J = 7.8 Hz, 2H), 6.58 (t, J = 7.3 Hz, 1H), 6.05 (d, J = 8.1 Hz, 1H), 5.17 (t, J = 5.8 Hz, 1H), 4.72 (m, 1H), 4.50 (d, J = 5.8 Hz, 2H), 4.28 (m, 1H), 2.62 (m, 1H), 2.14 (s, 3H), 1.25 (m, 1H), 1.10 (d, J = 6.4 Hz, 3H).

1-((2S*,4R*)-2-Methyl-6-(4-(morpholinomethyl)phenyl)-4-(phenylamino)-3,4-dihydroquinolin-1(2H)-yl)ethanone (23). N-((2S*,4R*)-1-Acetyl-6-(4-formylphenyl)-2-methyl-1,2,3,4-tetrahydroquinolin-4-yl)formamide (**58a**) was reacted with morpholine using method E. After formamide deprotection using method A, coupling of phenylboronic acid was carried out using method B; mp 80 °C. LCMS (method formate): retention time 1.18 min, [M + H]⁺ = 456.37. ¹H NMR (400 MHz, DMSO-*d*₆) δ 7.30–7.58 (m, 7H), 7.10 (d, J = 7.6 Hz, 2H), 6.72 (d, J = 7.6 Hz, 2H), 6.58 (t, J = 6.8 Hz, 1H), 6.05 (d, J = 7.6 Hz, 1H), 4.72 (m, 1H), 4.28 (m, 1H), 3.56 (m, 4H), 3.32 (br s, 2H), 2.62 (m, 1H), 2.35 (m, 4H), 2.14 (s, 3H), 1.25 (m, 1H), 1.10 (d, J = 5.6 Hz, 3H).

1-((2S*,4R*)-2-Methyl-4-(phenylamino)-6-(3-(piperidin-1-ylmethyl)phenyl)-3,4-dihydroquinolin-1(2H)-yl)ethanone (24). Suzuki coupling between N-((2S*,4R*)-1-acetyl-6-bromo-2-methyl-1,2,3,4-tetrahydroquinolin-4-yl)formamide (**54**) and (3-formylphenyl)boronic acid was carried out using method C. The resulting aldehyde was coupled with piperidine using method E. After formamide deprotection using method A, phenylboronic acid was coupled using method B. LCMS (method formate): retention time

1.41 min, $[M + H]^+$ = 454.31. ^1H NMR (400 MHz, $\text{DMSO}-d_6$) δ 7.49–7.69 (m, 2H), 7.31–7.48 (m, 4H), 7.22 (d, J = 7.3 Hz, 1H), 7.10 (dd, J = 7.8, 7.8 Hz, 2H), 6.72 (d, J = 7.8 Hz, 2H), 6.58 (t, J = 7.2 Hz, 1H), 6.07 (d, J = 8.1 Hz, 1H), 4.73 (m, 1H), 4.28 (m, 1H), 3.43 (s, 2H), 2.62 (m, 1H), 2.23–2.39 (m, 4H), 2.14 (s, 3H), 1.16–1.56 (m, 7H), 1.10 (d, J = 6.1 Hz, 3H).

1-((2S*,4R*)-2-Methyl-4-(phenylamino)-6-(4-(piperidin-1-ylmethyl)phenyl)-3,4-dihydroquinolin-1(2H)-yl)ethanone Hydrochloride (25). Method B was used starting from 1-((2S*,4R*)-4-amino-2-methyl-6-(4-(piperidin-1-ylmethyl)phenyl)-3,4-dihydroquinolin-1(2H)-yl)ethanone (27) and phenylboronic acid; mp 100 °C. LCMS (method formate): retention time 1.40 min, $[M + H]^+$ = 454.41. ^1H NMR (400 MHz, $\text{DMSO}-d_6$) δ 9.51 (br s, 1H), 7.38–7.68 (m, 7H), 7.11 (dd, J = 7.8, 7.8 Hz, 2H), 6.72 (d, J = 7.8 Hz, 2H), 6.58 (t, J = 7.2 Hz, 1H), 6.07 (d, J = 7.8 Hz, 1H), 4.72 (m, 1H), 4.28 (m, 3H), 2.88 (br s, 2H), 2.64 (m, 1H), 2.15 (s, 3H), 1.50–1.91 (m, 6H), 1.15–1.45 (m, 3H), 1.11 (d, J = 6.4 Hz, 3H).

N-((2S*,4R*)-1-Acetyl-2-methyl-6-(4-(piperidin-1-ylmethyl)phenyl)-1,2,3,4-tetrahydroquinolin-4-yl)formamide (26). Method E was used starting from N-((2S*,4R*)-1-acetyl-6-(4-formylphenyl)-2-methyl-1,2,3,4-tetrahydroquinolin-4-yl)formamide (58a) and piperidine. LCMS (method formate): retention time 1.03 min, $[M + H]^+$ = 406.24. ^1H NMR (400 MHz, $\text{DMSO}-d_6$) δ 8.57 (d, J = 8.3 Hz, 1H), 8.31 (s, 1H), 7.56–7.63 (m, 3H), 7.35–7.46 (m, 4H), 4.79 (m, 1H), 4.69 (m, 1H), 3.46 (s, 2H), 2.44–2.54 (m, 3H), 2.34 (m, 2H), 2.09 (s, 3H), 1.45–1.56 (m, 4H), 1.40 (m, 2H), 1.28 (m, 1H), 1.08 (d, J = 6.4 Hz, 3H).

1-((2S*,4R*)-4-Amino-2-methyl-6-(4-(piperidin-1-ylmethyl)phenyl)-3,4-dihydroquinolin-1(2H)-yl)ethanone (27). Formamide deprotection was carried out upon N-((2S*,4R*)-1-acetyl-2-methyl-6-(4-(piperidin-1-ylmethyl)phenyl)-1,2,3,4-tetrahydroquinolin-4-yl)formamide (26) using method A. LCMS (method formate): retention time 1.06 min, $[M + H]^+$ = 378.32. ^1H NMR (400 MHz, $\text{DMSO}-d_6$) δ 7.78 (br s, 1H), 7.65 (d, J = 8.1 Hz, 2H), 7.52 (dd, J = 1.7, 8.1 Hz, 1H), 7.38 (d, J = 8.1 Hz, 2H), 7.31 (d, J = 8.1 Hz, 1H), 4.62 (m, 1H), 3.59 (dd, J = 4.1, 11.9 Hz, 1H), 3.35 (m, 2H), 2.45 (m, 1H), 2.34 (m, 4H), 2.05 (s, 3H), 1.51 (m, 4H), 1.40 (m, 2H), 1.09 (d, J = 6.1 Hz, 3H), 1.05 (m, 1H). NH_2 not observed.

1-((2S,4R)-2-Methyl-4-(phenylamino)-6-(4-(piperidin-1-ylmethyl)phenyl)-3,4-dihydroquinolin-1(2H)-yl)ethanone (28) and 1-((2R,4S)-2-Methyl-4-(phenylamino)-6-(4-(piperidin-1-ylmethyl)phenyl)-3,4-dihydroquinolin-1(2H)-yl)ethanone (29). Compound 25 was dissolved in EtOH and separated in its two enantiomers using column CHIRALPAK AD 250 mm \times 4.6 mm 10 μm , eluting with hexane/EtOH 40/60 for 15 min at a concentration of 1 mg/mL to give 28 (retention time 4.7 min) and 29 (retention time 7.7 min).

Methyl 4-((2S*,4R*)-1-Acetyl-4-((4-(tert-butyl)phenyl)amino)-2-methyl-1,2,3,4-tetrahydroquinolin-6-yl)benzoate (30). Method B was used to couple methyl 4-((2S*,4R*)-1-acetyl-4-amino-2-methyl-1,2,3,4-tetrahydroquinolin-6-yl)benzoate (57a) and 4-(tert-butyl)phenylboronic acid; mp 144 °C. LCMS (method formate): retention time 1.43 min, $[M + H]^+$ = 471.39. ^1H NMR (400 MHz, $\text{DMSO}-d_6$) δ 8.00 (d, J = 8.3 Hz, 2H), 7.70 (d, J = 8.3 Hz, 2H), 7.63 (d, J = 8.1 Hz, 1H), 7.57 (br s, 1H), 7.46 (d, J = 8.1 Hz, 1H), 7.13 (d, J = 8.3 Hz, 2H), 6.68 (d, J = 8.3 Hz, 2H), 5.84 (d, J = 8.1 Hz, 1H), 4.71 (m, 1H), 4.28 (m, 1H), 3.86 (s, 3H), 2.62 (m, 1H), 2.15 (s, 3H), 1.29 (m, 1H), 1.22 (s, 9H), 1.10 (d, J = 6.1 Hz, 3H).

4-((2S*,4R*)-1-Acetyl-2-methyl-4-((4-(methylsulfonyl)phenyl)amino)-1,2,3,4-tetrahydroquinolin-6-yl)benzoic Acid (31). Method D was used to hydrolyze methyl 4-((2S*,4R*)-1-acetyl-2-methyl-4-((4-(methylsulfonyl)phenyl)amino)-1,2,3,4-tetrahydroquinolin-6-yl)benzoate (32). LCMS (method formate): retention time 0.62 min, $[M - H]^-$ = 477.39. ^1H NMR (400 MHz, $\text{DMSO}-d_6$) δ 12.00–13.65 (br s, 1H), 7.99 (d, J = 8.3 Hz, 2H), 7.59–7.69 (m, 5H), 7.49 (d, J = 8.3 Hz, 1H), 7.46 (d, J = 1.2 Hz, 1H), 7.06 (d, J = 8.1 Hz, 1H), 6.89 (d, J = 8.8 Hz, 2H), 4.74 (m, 1H), 4.53 (m, 1H), 3.01 (m, 3H), 2.64 (m, 1H), 2.16 (s, 3H), 1.32 (m, 1H), 1.12 (d, J = 6.1 Hz, 3H).

Methyl 4-((2S*,4R*)-1-Acetyl-2-methyl-4-((4-(methylsulfonyl)phenyl)amino)-1,2,3,4-tetrahydroquinolin-6-

yl)benzoate (32). Method B was used to couple methyl 4-((2S*,4R*)-1-acetyl-4-amino-2-methyl-1,2,3,4-tetrahydroquinolin-6-yl)benzoate (57a) and 4-(methylsulfonyl)phenylboronic acid. LCMS (method formate): retention time 1.04 min, $[M - H]^-$ = 491.43. ^1H NMR (400 MHz, $\text{DMSO}-d_6$) δ 8.01 (d, J = 8.3 Hz, 2H), 7.70 (d, J = 8.3 Hz, 2H), 7.66 (dd, J = 2.0, 8.3 Hz, 1H), 7.62 (d, J = 9.0 Hz, 2H), 7.50 (d, J = 8.3 Hz, 1H), 7.46 (d, J = 1.2 Hz, 1H), 7.06 (d, J = 8.1 Hz, 1H), 6.89 (d, J = 8.8 Hz, 2H), 4.73 (m, 1H), 4.51 (m, 1H), 3.86 (s, 3H), 3.32 (s, 3H), 2.64 (m, 1H), 2.16 (s, 3H), 1.29 (m, 1H), 1.12 (d, J = 6.4 Hz, 3H).

4-((2S*,4R*)-1-Acetyl-2-methyl-4-(p-tolylamino)-1,2,3,4-tetrahydroquinolin-6-yl)benzoic Acid (33). Method B was used to couple methyl 4-((2S*,4R*)-1-acetyl-4-amino-2-methyl-1,2,3,4-tetrahydroquinolin-6-yl)benzoate (57a) and 4-tolylboronic acid. This was followed by hydrolysis using method D. LCMS (method formate): retention time 0.73 min, $[M + H]^+$ = 415.36. ^1H NMR (400 MHz, $\text{DMSO}-d_6$) δ 11.90–13.70 (br s, 1H), 7.99 (d, J = 8.3 Hz, 2H), 7.66 (d, J = 8.3 Hz, 2H), 7.62 (dd, J = 1.8, 8.2 Hz, 1H), 7.53 (br s, 1H), 7.45 (s, J = 8.3 Hz, 1H), 6.92 (d, J = 8.3 Hz, 2H), 6.65 (d, J = 8.3 Hz, 2H), 5.84 (d, J = 8.1 Hz, 1H), 4.71 (m, 1H), 4.25 (m, 1H), 2.62 (m, 1H), 2.16 (s, 3H), 2.08 (s, 3H), 1.21 (m, 1H), 1.10 (d, J = 6.4 Hz, 3H).

4-((2S*,4R*)-1-Acetyl-4-((4-chlorophenyl)amino)-2-methyl-1,2,3,4-tetrahydroquinolin-6-yl)benzoic Acid (34). Method B was used to couple methyl 4-((2S*,4R*)-1-acetyl-4-amino-2-methyl-1,2,3,4-tetrahydroquinolin-6-yl)benzoate (57a) and 4-(chlorophenyl)boronic acid. This was followed by hydrolysis using method D; mp 84 °C. LCMS (method formate): retention time 1.08 min, $[M - H]^-$ = 433.15. ^1H NMR (400 MHz, $\text{DMSO}-d_6$) δ 12.76–13.15 (br s, 1H), 7.99 (d, J = 8.3 Hz, 2H), 7.67 (d, J = 8.3 Hz, 2H), 7.63 (m, 1H), 7.49 (m, 2H), 7.12 (d, J = 8.8 Hz, 2H), 6.74 (d, J = 8.8 Hz, 2H), 6.30 (d, J = 7.8 Hz, 1H), 4.71 (m, 1H), 4.30 (m, 1H), 2.62 (m, 1H), 2.15 (s, 3H), 1.23 (m, 1H), 1.10 (d, J = 6.1 Hz, 3H).

Methyl 4-((2S*,4R*)-1-Acetyl-4-((4-fluorophenyl)amino)-2-methyl-1,2,3,4-tetrahydroquinolin-6-yl)benzoate (35). Method B was used to couple methyl 4-((2S*,4R*)-1-acetyl-4-amino-2-methyl-1,2,3,4-tetrahydroquinolin-6-yl)benzoate (57a) and 4-(fluorophenyl)boronic acid. LCMS (method formate): retention time 1.19 min, $[M + H]^+$ = 433.23. ^1H NMR (300 MHz, CDCl_3) δ 8.09 (d, J = 8.16 Hz, 2H), 7.55–7.63 (m, 5H), 7.26 (m, 1H), 6.94 (m, 2H), 6.65 (m, 2H), 4.93 (m, 1H), 4.21 (m, 1H), 3.94 (s, 3H), 2.70 (m, 1H), 2.26 (s, 3H), 1.28–1.43 (m, 1H), 1.22 (d, J = 6.3 Hz, 3H).

4-((2S*,4R*)-1-Acetyl-4-((3-fluorophenyl)amino)-2-methyl-1,2,3,4-tetrahydroquinolin-6-yl)benzotrile (36). Method E was used starting from 1-((2S*,4R*)-4-amino-6-bromo-2-methyl-3,4-dihydroquinolin-1(2H)-yl)ethanone (55) and 4-(cyanophenyl)boronic acid; then method B was used with (3-fluorophenyl)boronic acid; mp 124 °C. LCMS (method formate): retention time 1.20 min, $[M + H]^+$ = 400.30. ^1H NMR (400 MHz, $\text{DMSO}-d_6$) δ 7.90 (d, J = 8.3 Hz, 2H), 7.75 (d, J = 8.3 Hz, 2H), 7.66 (dd, J = 2.0, 8.3 Hz, 1H), 7.46–7.51 (m, 2H), 7.11 (dd, J = 7.6, 7.6 Hz, 1H), 6.51–6.61 (m, 2H), 6.40 (d, J = 8.1 Hz, 1H), 6.34 (ddd, J = 2.0, 7.6, 7.6 Hz, 1H), 4.70 (m, 1H), 4.32 (m, 1H), 2.62 (m, 1H), 2.15 (s, 3H), 1.23 (m, 1H), 1.10 (d, J = 6.4 Hz, 3H).

4-((2S*,4R*)-1-Acetyl-4-((3-methoxyphenyl)amino)-2-methyl-1,2,3,4-tetrahydroquinolin-6-yl)benzotrile (37). Method E was used starting from 1-((2S*,4R*)-4-amino-6-bromo-2-methyl-3,4-dihydroquinolin-1(2H)-yl)ethanone (55) and 4-(cyanophenyl)boronic acid; then method B was used with (3-methoxyphenyl)boronic acid; mp 104 °C. LCMS (method formate): retention time 1.17 min, $[M + H]^+$ = 412.26. ^1H NMR (400 MHz, $\text{DMSO}-d_6$) δ 7.90 (d, J = 8.3 Hz, 2H), 7.75 (d, J = 8.3 Hz, 2H), 7.65 (dd, J = 2.0, 8.1 Hz, 1H), 7.53 (d, J = 1.2 Hz, 1H), 7.48 (d, J = 8.1 Hz, 1H), 7.01 (t, J = 8.1 Hz, 1H), 6.28–6.36 (m, 2H), 6.19 (dd, J = 2.0, 8.1 Hz, 1H), 6.06 (d, J = 8.3 Hz, 1H), 4.70 (m, 1H), 4.32 (m, 1H), 3.31 (s, 3H), 2.62 (m, 1H), 2.13 (s, 3H), 1.24 (m, 1H), 1.10 (d, J = 6.4 Hz, 3H).

4-((2S*,4R*)-1-Acetyl-4-((3-methoxyphenyl)amino)-2-methyl-1,2,3,4-tetrahydroquinolin-6-yl)benzoic Acid (38). Method B was used starting from methyl 4-((2S*,4R*)-1-acetyl-4-amino-2-methyl-1,2,3,4-tetrahydroquinolin-6-yl)benzoate (57a) and (3-methoxyphenyl)boronic acid. This was followed by hydrolysis using

method D; mp 148 °C. LCMS (method formate): retention time 0.69 min, $[M + H]^+ = 431.31$. $^1\text{H NMR}$ (400 MHz, DMSO- d_6) δ 7.99 (d, $J = 8.1$ Hz, 2H), 7.67 (d, $J = 8.3$ Hz, 2H), 7.62 (d, $J = 8.1$ Hz, 1H), 7.54 (br s, 1H), 7.45 (d, $J = 8.3$ Hz, 1H), 7.01 (dd, $J = 8.1, 8.1$ Hz, 1H), 6.29–6.36 (m, 2H), 6.19 (d, $J = 8.1$ Hz, 1H), 6.07 (d, $J = 8.1$ Hz, 1H), 4.71 (m, 1H), 4.31 (m, 1H), 3.67 (s, 3H), 2.62 (m, 1H), 2.15 (s, 3H), 1.22 (m, 1H), 1.10 (d, $J = 6.4$ Hz, 3H). CO_2H not observed.

4-((2S*,4R*)-1-Acetyl-4-((2-methoxyphenyl)amino)-2-methyl-1,2,3,4-tetrahydroquinolin-6-yl)benzoic Acid (39). Method B was used starting from methyl 4-((2S*,4R*)-1-acetyl-4-amino-2-methyl-1,2,3,4-tetrahydroquinolin-6-yl)benzoate (57a) and (2-methoxyphenyl)boronic acid. This was followed by hydrolysis using method D. LCMS (method formate): retention time 0.72 min, $[M + H]^+ = 431.34$. $^1\text{H NMR}$ (400 MHz, DMSO- d_6) δ 12.05–13.82 (br s, 1H), 7.97 (d, $J = 8.3$ Hz, 2H), 7.58–7.65 (m, 3H), 7.45 (d, $J = 8.1$ Hz, 1H), 7.41 (br s, 1H), 6.90 (d, $J = 7.8$ Hz, 1H), 6.75 (t, $J = 7.8$ Hz, 1H), 6.63 (m, 2H), 5.10 (d, $J = 8.1$ Hz, 1H), 4.72 (m, 1H), 4.31 (m, 1H), 3.85 (s, 3H), 2.61 (m, 1H), 2.15 (s, 3H), 1.43 (m, 1H), 1.10 (d, $J = 6.4$ Hz, 3H).

1-((2S*,4R*)-4-((4-Chlorophenyl)amino)-2-methyl-6-(4-(piperidin-1-ylmethyl)phenyl)-3,4-dihydroquinolin-1(2H)-yl)ethanone (40). Method B was used to couple 1-((2S*,4R*)-4-amino-2-methyl-6-(4-(piperidin-1-ylmethyl)phenyl)-3,4-dihydroquinolin-1(2H)-yl)ethanone (27) and (4-chlorophenyl)boronic acid; mp 128 °C. LCMS (method formate): retention time 1.49 min, $[M + H]^+ = 490.31$. $^1\text{H NMR}$ (400 MHz, DMSO- d_6) δ 7.28–7.60 (m, 7H), 7.12 (d, $J = 8.6$ Hz, 2H), 6.73 (d, $J = 8.6$ Hz, 2H), 6.28 (d, $J = 8.1$ Hz, 1H), 4.72 (m, 1H), 4.28 (m, 1H), 3.45 (br s, 2H), 2.61 (m, 1H), 2.35 (m, 4H), 2.14 (s, 3H), 1.50 (m, 4H), 1.40 (m, 2H), 1.24 (m, 1H), 1.09 (d, $J = 6.1$ Hz, 3H).

3-(1-Acetyl-4-((4-chlorophenyl)amino)-2-methyl-1,2,3,4-tetrahydroquinolin-6-yl)benzoic Acid (41). Hydrolysis of 42 was carried out using method D; mp 152 °C. LCMS (method formate): retention time 0.79 min, $[M - H]^- = 433.35$. $^1\text{H NMR}$ (400 MHz, DMSO- d_6) δ 12.74–13.20 (br s, 1H), 8.10 (s, 1H), 7.90 (dd, $J = 1.2, 7.8$ Hz, 1H), 7.80 (t, $J = 7.8$ Hz, 1H), 7.53–7.64 (m, 2H), 7.41–7.50 (m, 2H), 7.12 (d, $J = 9.0$ Hz, 2H), 6.74 (d, $J = 9.0$ Hz, 2H), 6.31 (d, $J = 8.1$ Hz, 1H), 4.72 (m, 1H), 4.30 (m, 1H), 2.62 (m, 1H), 2.15 (s, 3H), 1.24 (m, 1H), 1.10 (d, $J = 6.4$ Hz, 3H).

Methyl 3-((2S*,4R*)-1-Acetyl-4-((4-chlorophenyl)amino)-2-methyl-1,2,3,4-tetrahydroquinolin-6-yl)benzoate (42). Method B was used starting from 1-((2S*,4R*)-4-amino-6-bromo-2-methyl-3,4-dihydroquinolin-1(2H)-yl)ethanone (55) and (4-chlorophenyl)boronic acid. Suzuki coupling with (3-(methoxycarbonyl)phenyl)boronic acid was then effected using method C; mp 98 °C. LCMS (method formate): retention time 1.31 min, $[M - H]^- = 447.34$. $^1\text{H NMR}$ (400 MHz, DMSO- d_6) δ 8.07 (s, 1H), 7.92 (dd, $J = 1.2, 7.8$ Hz, 1H), 7.80 (d, $J = 7.8$ Hz, 1H), 7.52–7.66 (m, 2H), 7.45 (d, $J = 9.0$ Hz, 2H), 7.13 (d, $J = 9.0$ Hz, 2H), 6.74 (d, $J = 9.1$ Hz, 2H), 6.32 (d, $J = 8.1$ Hz, 1H), 4.71 (m, 1H), 4.30 (m, 1H), 3.87 (s, 3H), 2.62 (m, 1H), 2.15 (s, 3H), 1.25 (m, 1H), 1.10 (d, $J = 6.4$ Hz, 3H).

4-((2S*,4R*)-1-Acetyl-4-((4-chlorophenyl)amino)-2-methyl-1,2,3,4-tetrahydroquinolin-6-yl)benzamide (43). A solution of 4-((2S*,4R*)-1-acetyl-4-((4-chlorophenyl)amino)-2-methyl-1,2,3,4-tetrahydroquinolin-6-yl)benzoic acid (34) (250 mg, 0.575 mmol) in DMF (5 mL) at room temperature was treated with EDCI (220 mg, 1.15 mmol), HOBT (116 mg, 0.862 mmol), and NEt_3 (0.16 mL, 1.15 mmol). The resulting mixture was stirred at this temperature for 15 min then treated with a 25% w/w NH_4OH aqueous solution (0.06 mL, 1.15 mmol). After continued stirring at this temperature for 16 h, more EDCI (50 mg, 0.26 mmol) and 25% w/w NH_4OH aqueous solution (0.06 mL, 1.15 mmol) were added and the mixture was stirred for another 2 h, then was concentrated in vacuo. The residue was dissolved in EtOAc, and the organic phase was washed successively with a 0.5N NaOH aqueous solution, a 0.5 N HCl aqueous solution, water and brine, then dried over Na_2SO_4 and concentrated in vacuo. Purification of the residue by flash chromatography on silica gel (5% MeOH in CH_2Cl_2) and recrystallization in EtOH gave 43 (82 mg, 33%) as white crystals; mp 235 °C. LCMS (method formate): retention time 1.00 min, $[M + H]^+ = 434.27$. $^1\text{H NMR}$ (400 MHz,

DMSO- d_6) δ 7.96 (br s, 1H), 7.93 (d, $J = 8.6$ Hz, 2H), 7.63 (d, $J = 2.0$ Hz, 1H), 7.61 (d, $J = 8.3$ Hz, 2H), 7.46 (m, 2H), 7.35 (br s, 1H), 7.13 (d, $J = 7.8$ Hz, 2H), 6.75 (d, $J = 7.8$ Hz, 2H), 6.28 (d, $J = 8.1$ Hz, 1H), 4.72 (m, 1H), 4.31 (m, 1H), 2.62 (m, 1H), 2.15 (s, 3H), 1.23 (m, 1H), 1.10 (d, $J = 6.4$ Hz, 3H).

1-((2S*,4R*)-4-((4-Chlorophenyl)amino)-2-methyl-6-(o-tolyl)-3,4-dihydroquinolin-1(2H)-yl)ethanone (44). Method C was used starting from 1-((2S*,4R*)-6-bromo-4-((4-chlorophenyl)amino)-2-methyl-3,4-dihydroquinolin-1(2H)-yl)ethanone (56a) and o-tolylboronic acid. LCMS (method formate): retention time 1.39 min, $[M + H]^+ = 405.32$. $^1\text{H NMR}$ (300 MHz, CDCl_3) δ 7.08–7.34 (m, 11H), 6.59 (d, $J = 8.2$ Hz, 1H), 4.94 (m, 1H), 4.23 (m, 1H), 2.70 (m, 1H), 2.28 (s, 3H), 2.19 (s, 3H), 1.30 (m, 1H), 1.23 (d, $J = 6.3$ Hz, 3H).

(R)-1-(6-(4-Methoxyphenyl)-4-(phenylamino)-3,4-dihydroquinolin-1(2H)-yl)ethanone (45). To a solution of 1-acetyl-6-(4-methoxyphenyl)-2,3-dihydroquinolin-4(1H)-one (62) (280 mg, 0.95 mmol), aniline (0.25 mL, 2.85 mmol), and NEt_3 (0.67 mL, 4.75 mmol) in anhydrous CH_2Cl_2 (10 mL) at 0 °C was added dropwise a 1.0 M solution of titanium tetrachloride in CH_2Cl_2 (0.95 mL, 0.95 mmol). After stirring 18 h at room temperature, the reaction mixture was poured into water and extracted with CH_2Cl_2 . The organic phase was dried over Na_2SO_4 , filtered, and evaporated to dryness. The residue was taken up in $i\text{Pr}_2\text{O}$, and the filtrate was evaporated to dryness and directly dissolved in AcOH. $\text{NaB}(\text{OAc})_3\text{H}$ was added portionwise, then the reaction mixture was stirred for 18 h and basified with concentrated NaOH aqueous solution. The aqueous solution was extracted with CH_2Cl_2 and washed with brine, dried over Na_2SO_4 , filtered, and evaporated to dryness. The residue was purified by flash chromatography on silica gel (CH_2Cl_2), and the resulting solid was recrystallized in CH_3CN to deliver the title compound (65 mg, 15%) as a white powder. LCMS (method formate): retention time 1.22 min, $[M + H]^+ = 373.27$. $^1\text{H NMR}$ (400 MHz, DMSO- d_6) δ 7.42–7.56 (m, 5H), 7.11 (dd, $J = 7.9, 7.9$ Hz, 2H), 6.99 (d, $J = 8.8$ Hz, 2H), 6.74 (d, $J = 7.8$ Hz, 2H), 6.57 (t, $J = 7.3$ Hz, 1H), 6.07 (d, $J = 8.3$ Hz, 1H), 4.56 (m, 1H), 4.02 (m, 1H), 3.58 (m, 1H), 3.32 (s, 3H), 2.24 (s, 3H), 2.22 (m, 1H), 1.82 (m, 1H).

4-((2S,4R)-1-Acetyl-2-methyl-4-(p-tolylamino)-1,2,3,4-tetrahydroquinolin-6-yl)benzoic Acid (46). Compound 46 can be obtained in a similar manner to compound 33 from the single enantiomer of compound 57a, which can be obtained from the racemate as follows: A solution of methyl 4-((1-acetyl-4-amino-2-methyl-1,2,3,4-tetrahydroquinolin-6-yl)benzoate (57a) (103 g, 0.305 mol) in EtOH (500 mL) was treated with L-(+)-lactic acid (20% w/w solution in water, 260 mL, 0.610 mmol), and the resulting mixture was refluxed for 30 min then cooled to room temperature and concentrated in vacuo. The residue was suspended in hexane (160 mL) and triturated at reflux for 10 min. The mixture was cooled to room temperature, the solid filtered off, and the trituration in hexane repeated once. The solid obtained was suspended in EtOAc (1.3 L) and triturated at reflux for 30 min to give a white precipitate. The mixture was then cooled to room temperature and left still for 16 h. The solid was filtered off and rinsed with EtOAc. The filtrate was treated with a saturated Na_2CO_3 aqueous solution, and the resulting mixture was stirred for 30 min. The aqueous phase was extracted with AcOEt (1.5 L) and CH_2Cl_2 (1 L), and the combined organics were dried over Na_2SO_4 and concentrated in vacuo to give 50.3 g of amine. This residue was dissolved in THF (500 mL) and treated with L-(–)-dibenzoyltartaric acid (26.7 g, 74.6 mmol), and the resulting mixture was refluxed for 20 min then was cooled to room temperature and left still for 72 h then at 0 °C for 30 min. The precipitate obtained was filtered off and rinsed with THF (100 mL). This precipitate was refluxed in EtOH (1.1 L), and the mixture was left at room temperature for 16 h then at 0 °C for 30 min. The solid was filtered off and dried under vacuum. It was then basified with a saturated Na_2CO_3 aqueous solution. The aqueous phase was extracted with CH_2Cl_2 (3 L overall), and the organic phase was dried over Na_2SO_4 and concentrated in vacuo to give methyl 4-((2S,4R)-1-acetyl-4-amino-2-methyl-1,2,3,4-tetrahydroquinolin-6-yl)benzoate (28.6 g, 28%, ee >99.5%) as a white solid.

4-((2S,4R)-1-Acetyl-4-((4-chlorophenyl)amino)-2-methyl-1,2,3,4-tetrahydroquinolin-6-yl)benzoic Acid (47). A solution of ethyl 4-((2S,4R)-1-acetyl-4-((4-chlorophenyl)amino)-2-methyl-1,2,3,4-tetrahydro-6-quinolinyl)benzoate (**69**) (28.0 g, 60.5 mmol) in EtOH (380 mL) at room temperature was treated with a 2 M NaOH aqueous solution (190 mL, 60.5 mmol). The resulting mixture was stirred at this temperature for 3 h. Most of EtOH was removed in vacuo. The resulting orange emulsion was diluted with water, and the aqueous phase was extracted twice with CH₂Cl₂. The combined organic phases were washed with water, and the combined aqueous phases were acidified with a 2 N HCl aqueous solution. The aqueous phase was then extracted twice with EtOAc. The combined organic phases were dried over MgSO₄ and concentrated in vacuo. The residual orange foam was suspended in EtOAc, and the resulting mixture was stirred at room temperature for 15 min. The solid formed was filtered off, rinsed with EtOAc, and dried under vacuum at 50 °C to give **47** (20.2 g, 77%) as a cream solid. ¹H NMR, ¹³C NMR, and chiral analysis of the product showed no evidence of epimerization, ee >99%. LCMS (method formate): retention time 1.08 min, [M - H]⁻ = 433.15. ¹H NMR (600 MHz, DMSO-*d*₆) δ ppm 12.92 (br s, 1H), 8.00–7.97 (m, 2H), 7.68–7.65 (m, 2H), 7.63 (dd, *J* = 8.2, 2.1 Hz, 1H), 7.48 (d, *J* = 1.5 Hz, 1H), 7.46 (d, *J* = 8.1 Hz, 1H), 7.19–7.09 (m, 2H), 6.70–6.78 (m, 2H), 6.26 (d, *J* = 8.1 Hz, 1H), 4.66–4.77 (m, 1H), 4.30 (ddd, *J* = 11.8, 7.9, 4.1 Hz, 1H), 2.62 (ddd, *J* = 12.5, 8.4, 4.2 Hz, 1H), 2.15 (s, 3H), 1.27–1.20 (m, 1H), 1.10 (d, *J* = 6.2 Hz, 3H). ¹³C NMR (150.9 MHz, DMSO-*d*₆) δ ppm 168.6 (s, 1C), 167.0 (s, 1C), 147.1 (s, 1C), 143.9 (s, 1C), 137.9 (s, 1C), 136.7 (s, 1C), 135.8 (s, 1C), 130.0 (s, 2C), 129.5 (s, 1C), 128.7 (s, 2C), 126.6 (s, 1C), 126.5 (s, 2C), 125.3 (s, 1C), 121.8 (s, 1C), 119.5 (s, 1C), 114.1 (s, 2C), 48.8 (s, 1C), 47.2 (s, 1C), 39.9 (s, 1C), 22.9 (s, 1C), 21.3 (s, 1C). See Supporting Information Figure S4 for NMR spectra. [α]_D = +40.8° (*T* = 21.4 °C, 10 mm cell, *c* = 10 mg/mL, MeOH).

3-(Phenylamino)butanoic Acid (49). A solution of aniline (93.3 g, 1 mol) and crotonic acid (66 g, 0.77 mol) in toluene (600 mL) was heated to reflux. After 24 h, the reaction mixture was evaporated to dryness and the residue was purified by flash chromatography on silica gel to afford intermediate **49** as a brown oil (77.5 g, 43%). ¹H NMR (300 MHz, CDCl₃) δ ppm 7.23 (t, *J* = 7.6 Hz, 2H), 6.81 (t, *J* = 7.6 Hz, 1H), 6.73 (d, *J* = 7.6 Hz, 2H), 3.95 (m, 1H), 2.70 (m, 1H), 2.55 (m, 1H), 1.32 (d, *J* = 6.6 Hz, 3H).

2-Methyl-2,3-dihydroquinolin-4(1H)-one (50). A mixture of 3-(phenylamino)butanoic acid (**49**) (30 g, 0.168 mol) and PPA (300 mL) was heated to 110 °C. After 5 h, the reaction mixture was poured into ice and a saturated aqueous solution of NaHCO₃ was added until pH 7. The aqueous layer was extracted with EtOAc (3 × 1 L). The combined organic layers were washed with brine and dried over Na₂SO₄ and concentrated under reduced pressure. The residue was purified by flash chromatography on silica gel (8 g, 29%). ¹H NMR (300 MHz, CDCl₃) δ ppm 7.74 (dd, *J* = 1.5 and 7.9 Hz, 1H), 7.25 (m, 1H), 6.66 (m, 1H), 6.57 (d, *J* = 7.9 Hz, 1H), 3.70 (m, 1H), 2.55 (dd, *J* = 3.8 and 16.1 Hz, 1H), 2.44 (dd, *J* = 13.0 and 16.1 Hz, 1H), 1.27 (d, *J* = 6.4 Hz, 3H).

1-Acetyl-2-methyl-2,3-dihydroquinolin-4(1H)-one (51). To a solution of 2-methyl-2,3-dihydroquinolin-4(1H)-one (**50**) (6.44 g, 40 mmol) in anhydrous CH₂Cl₂ (150 mL) at 0 °C was added acetyl chloride (3.45 g, 45 mmol) followed by DMAP (0.48 g, 4 mmol). The mixture was stirred for 18 h at room temperature, and then 1N NaOH was added until pH 7–8. The organic layer was separated, dried over Na₂SO₄, and concentrated under reduced pressure. The residue was taken up in pentane, filtered, then washed with iPr₂O to deliver intermediate **51** as an off-white powder (6.95 g, 86%). LCMS (method formate): retention time 2.12 min. [M + H]⁺ = 204.0. ¹H NMR (300 MHz, CDCl₃) δ ppm 8.01 (dd, *J* = 1.7 and 7.7 Hz, 1H), 7.57 (m, 1H), 7.39 (br s, 1H), 7.28 (m, 1H), 5.35 (br s, 1H), 3.05 (dd, *J* = 5.8 and 17.9 Hz, 1H), 2.58 (dd, *J* = 1.7 and 17.9 Hz, 1H), 2.35 (s, 3H), 1.21 (d, *J* = 7.0 Hz, 3H).

N-(1-(1H-Benzo[d][1,2,3]triazol-1-yl)ethyl)-4-bromoaniline (52). To a suspension of benzotriazole (139 g, 1.16 mol) in toluene (2 L) in a 3 L, four-neck flask under nitrogen atmosphere was added at room temperature a solution of 4-bromoaniline (200 g, 1.16 mol) in

toluene (300 mL). Acetaldehyde (64.7 mL, 1.17 mol) in solution in toluene (200 mL) was added dropwise. The reaction mixture became progressively homogeneous and then gave a precipitate. The resulting mixture was stirred 12 h under nitrogen atmosphere then filtered. The precipitate was recrystallized in toluene to afford intermediate **52** as a white solid (304 g, 82%). ¹H NMR (400 MHz, DMSO-*d*₆) δ 8.10 (d, *J* = 8.6 Hz, 1H), 8.00 (d, *J* = 8.6 Hz, 1H), 7.51 (m, 2H), 7.43 (m, 1H), 7.16 (d, *J* = 8.2 Hz, 2H), 6.63 (d, *J* = 8.2 Hz, 2H), 1.86 (d, *J* = 6.8 Hz, 3H). NH not observed.

N-((2S*,4R*)-6-Bromo-2-methyl-1,2,3,4-tetrahydroquinolin-4-yl)formamide (53). A 3 L, four-neck flask under nitrogen atmosphere was charged with *N*-vinyl formamide (66.2 g, 0.946 mol) and dry THF (400 mL). BF₃·Et₂O (239 mL, 1.9 mol) was added dropwise at –5 °C to the milky mixture. After 15 min, **52** (150 g, 0.473 mol) in solution in THF (1 L) was added at –5 °C. After 2 h, the mixture was slowly and carefully poured in a NaHCO₃ saturated aqueous solution (5 L). EtOAc (2 L) was added, and the mixture was transferred to a separatory funnel. The organic layer was separated and was washed with water (1 × 200 mL) and brine (1 × 200 mL) and dried over Na₂SO₄. The mixture was filtered and the solid washed with EtOAc (1 × 50 mL). The filtrate was concentrated progressively until a precipitate appeared and the mixture cooled in an ice bath for 2 h. The precipitate was filtered through a Buchner funnel and washed with iPr₂O (2 × 100 mL) to deliver intermediate **53** (71 g, 56%) as a solid. LCMS (method formate): retention time 0.79 min, [M + H]⁺ = 269.05, 272.18 (1 Br). ¹H NMR (400 MHz, DMSO-*d*₆) δ 8.37 (d, *J* = 8.8 Hz, 1H), 8.21 (s, 1H), 7.05 (dd, *J* = 2.1, 8.4 Hz, 1H), 6.97 (s, 1H), 6.44 (d, *J* = 8.8 Hz, 1H), 5.93 (s, 1H), 5.10 (m, 1H), 3.41 (m, 1H), 1.95 (m, 1H), 1.40 (m, 1H), 1.14 (d, *J* = 6.4 Hz, 3H).

N-((2S*,4R*)-1-Acetyl-6-bromo-2-methyl-1,2,3,4-tetrahydroquinolin-4-yl)formamide (54). Acetyl chloride (21 mL, 0.29 mol) was added dropwise at 0 °C to a solution of **53** (71 g, 0.26 mol) in a mixture of CH₂Cl₂ (1 L) and pyridine (350 mL). After stirring 2 h at 0 °C, the mixture was poured into a mixture of crushed ice (2 kg) and concentrated HCl (450 mL). The product was extracted with CH₂Cl₂ (1 L), washed with brine, and dried over Na₂SO₄. Concentration under vacuum afforded intermediate **54** (82 g, 100%) as an off-white solid. LCMS (method formate): retention time 0.73 min, [M + H]⁺ = 311.08, 313.04 (1 Br). ¹H NMR (400 MHz, DMSO-*d*₆) δ 8.53 (d, *J* = 8.3 Hz, 1H), 8.27 (s, 1H), 7.49 (dd, *J* = 1.8, 8.4 Hz, 1H), 7.29–7.34 (m, 2H), 4.58–4.77 (m, 2H), 2.45 (m, 1H), 2.08 (s, 3H), 1.25 (m, 1H), 1.05 (m, 3H).

1-((2S*,4R*)-4-Amino-6-bromo-2-methyl-3,4-dihydroquinolin-1(2H)-yl)ethanone Hydrochloride (55). Method A was used starting from *N*-((2S*,4R*)-1-acetyl-6-bromo-2-methyl-1,2,3,4-tetrahydroquinolin-4-yl)formamide (**54**). Yield: 91% (oil). LCMS (method formate): retention time 0.76 min, [M + H]⁺ = 283.285 (1 Br). ¹H NMR (400 MHz, DMSO-*d*₆) δ 9.03 (br s, 3H), 7.61 (d, *J* = 1.5 Hz, 1H), 7.58 (dd, *J* = 1.5, 8.3 Hz, 1H), 7.37 (d, *J* = 8.3 Hz, 1H), 4.56–4.72 (m, 1H), 4.13–4.30 (m, 1H), 2.74 (m, 1H), 2.04 (s, 3H), 1.25–1.41 (m, 1H), 1.06 (d, *J* = 6.36 Hz, 3H).

1-((2S*,4R*)-6-Bromo-2-methyl-4-(phenylamino)-3,4-dihydroquinolin-1(2H)-yl)ethanone (56). Method B was used starting from 1-((2S*,4R*)-4-amino-6-bromo-2-methyl-3,4-dihydroquinolin-1(2H)-yl)ethanone hydrochloride (**55**) and phenylboronic acid. LCMS (method formate): retention time 1.20 min, [M + H]⁺ = 359.36 (1 Br). ¹H NMR (400 MHz, DMSO-*d*₆) δ 7.45 (dd, *J* = 2.0, 8.4 Hz, 1H), 7.31 (d, *J* = 8.4 Hz, 1H), 7.24 (d, *J* = 2.0 Hz, 1H), 7.11 (dd, *J* = 7.3, 8.4 Hz, 2H), 6.67 (d, *J* = 8.4 Hz, 2H), 6.59 (t, *J* = 7.3 Hz, 1H), 6.06 (d, *J* = 7.8 Hz, 1H), 4.67 (m, 1H), 4.22 (m, 1H), 2.58 (m, 1H), 2.08 (s, 3H), 1.19 (m, 1H), 1.06 (d, *J* = 6.4 Hz, 3H).

1-((2S*,4R*)-6-Bromo-4-((4-chlorophenyl)amino)-2-methyl-3,4-dihydroquinolin-1(2H)-yl)ethanone (56a). Method B was used starting from 1-((2S*,4R*)-4-amino-6-bromo-2-methyl-3,4-dihydroquinolin-1(2H)-yl)ethanone (**55**) and (4-chlorophenyl)boronic acid. LCMS (method formate): retention time 1.28 min, [M + H]⁺ = 393.14, 395.01 (1 Br). ¹H NMR (400 MHz, DMSO-*d*₆) δ 7.45 (dd, *J* = 1.7, 8.3 Hz, 1H), 7.31 (d, *J* = 8.3 Hz, 1H), 7.20 (d, *J* = 1.7 Hz, 1H), 7.12 (d, *J* = 8.9 Hz, 2H), 6.69 (d, *J* = 8.9 Hz, 2H), 6.28 (d, *J* = 7.8 Hz,

1H), 4.67 (m, 1H), 4.23 (m, 1H), 2.58 (m, 1H), 2.07 (s, 3H), 1.17 (m, 1H), 1.06 (d, $J = 6.4$ Hz, 3H).

Methyl 4-((2S*,4R*)-1-Acetyl-4-amino-2-methyl-1,2,3,4-tetrahydroquinolin-6-yl)benzoate (57a). Method B was used to couple (4-(methoxycarbonyl)phenyl)boronic acid to *N*-((2S*,4R*)-1-acetyl-6-bromo-2-methyl-1,2,3,4-tetrahydroquinolin-4-yl)formamide (54) before formamide deprotection using method A; mp 250 °C. LCMS (method formate): retention time 0.89 min, $[M + H]^+ = 339.25$. ¹H NMR (400 MHz, DMSO-*d*₆) δ 8.06 (d, $J = 8.1$ Hz, 2H), 7.86–7.90 (m, 3H), 7.62 (dd, $J = 2.0, 8.3$ Hz, 1H), 7.38 (d, $J = 8.3$ Hz, 1H), 4.62 (m, 1H), 3.88 (s, 3H), 3.61 (dd, $J = 4.2, 12.0$ Hz, 1H), 2.44 (m, 1H), 2.08 (s, 3H), 1.05 (d, $J = 6.4$ Hz, 3H), 1.02 (m, 1H). NH₂ not observed.

***N*-((2S*,4R*)-1-Acetyl-6-(4-formylphenyl)-2-methyl-1,2,3,4-tetrahydroquinolin-4-yl)formamide (58a).** Method C was used starting from *N*-((2S*,4R*)-1-acetyl-6-bromo-2-methyl-1,2,3,4-tetrahydroquinolin-4-yl)formamide (54) and (4-formylphenyl)boronic acid; mp 86 °C. LCMS (method formate): retention time 0.78 min, $[M + H]^+ = 337.24$. ¹H NMR (400 MHz, DMSO-*d*₆) δ 10.06 (s, 1H), 8.75 (d, $J = 8.6$ Hz, 1H), 8.31 (s, 1H), 8.01 (d, $J = 8.1$ Hz, 2H), 7.93 (d, $J = 8.1$, 2H), 7.71 (dd, $J = 1.5, 8.2$ Hz, 1H), 7.58 (d, $J = 1.5$ Hz, 1H), 7.49 (d, $J = 8.2$ Hz, 1H), 4.82 (m, 1H), 4.69 (m, 1H), 2.51 (m, 1H), 2.12 (s, 3H), 1.30 (m, 1H), 1.05–1.11 (d, $J = 6.4$ Hz, 3H).

***N*-((2S*,4R*)-1-Acetyl-2-methyl-6-(4-(piperidin-1-yl)methyl)phenyl)-1,2,3,4-tetrahydroquinolin-4-yl)formamide (59).** Method E was used starting from *N*-((2S*,4R*)-1-acetyl-6-(4-formylphenyl)-2-methyl-1,2,3,4-tetrahydroquinolin-4-yl)formamide (58a) and piperidine. LCMS (method formate): retention time 1.03 min, $[M + H]^+ = 406.24$. ¹H NMR (400 MHz, DMSO-*d*₆) δ 8.57 (d, $J = 8.3$ Hz, 1H), 8.31 (s, 1H), 7.56–7.63 (m, 3H), 7.35–7.46 (m, 4H), 4.79 (m, 1H), 4.69 (m, 1H), 3.46 (s, 2H), 2.44–2.54 (m, 3H), 2.34 (m, 2H), 2.09 (s, 3H), 1.45–1.56 (m, 4H), 1.40 (m, 2H), 1.28 (m, 1H), 1.08 (d, $J = 6.4$ Hz, 3H).

6-Bromo-2,3-dihydroquinolin-4(1H)-one (60). To a solution of 2,3-dihydroquinolin-4(1H)-one (1.85 g, 12.6 mmol) in CH₂Cl₂ (15 mL) at 0 °C was added *N*-bromosuccinimide (2.28 g, 12.8 mmol), and the mixture was stirred for 1.5 h. CH₂Cl₂ was added to the reaction mixture, then the organic layer was separated and washed with 1N NaOH aqueous solution and brine and dried over Na₂SO₄. The residue was purified by flash chromatography on silica gel (0–1% MeOH in CH₂Cl₂) to afford 6-bromo-2,3-dihydroquinolin-4(1H)-one (60) (2.43 g, 86%) as a yellow solid. LCMS (method formate, 5 min): retention time 2.52 min, $[M + H]^+ = 225.23$. ¹H NMR (300 MHz, CDCl₃) δ ppm 7.87 (d, $J = 2.5$ Hz, 1H), 7.27 (dd, $J = 2.3$ and 8.7 Hz, 1H), 6.53 (d, $J = 8.7$ Hz, 1H), 3.51 (t, $J = 6.8$ Hz, 2H), 2.62 (t, $J = 6.8$ Hz, 2H).

1-Acetyl-6-bromo-2,3-dihydroquinolin-4(1H)-one (61). A mixture of 6-bromo-2,3-dihydroquinolin-4(1H)-one (60) (1.10 g, 4.9 mmol) and acetic anhydride (11 mL) was stirred for 2 h at 80 °C and 15 h at 40 °C then concentrated under reduced pressure. The residue was recrystallized in acetonitrile to deliver 61 (0.91 g, 69%) as pale-yellow solid. LCMS (method formate, 5 min): retention time 2.44 min, $[M + H]^+ = 268.00$. ¹H NMR (300 MHz, DMSO) δ ppm 7.90 (s, 1H), 7.75 (m, 2H), 4.12 (t, $J = 6.1$ Hz, 2H), 2.81 (t, $J = 6.1$ Hz, 2H), 2.30 (s, 3H).

1-Acetyl-6-(4-methoxyphenyl)-2,3-dihydroquinolin-4(1H)-one (62). To a solution of 1-acetyl-6-bromo-2,3-dihydroquinolin-4(1H)-one (61) (0.91 g, 3.4 mmol) in 1,2-dimethoxyethane (25 mL) was added (4-methoxyphenyl)boronic acid (0.67 g, 4.4 mmol), a 2.5 M solution of cesium carbonate in water (3.4 mL, 3.5 mmol) and Pd(PPh₃)₄ (0.11 g, 0.035 mmol), and the mixture was stirred under reflux for 3.3 h. The solvent was then removed under reduced pressure, and CH₂Cl₂ was added to the residue. The organic phase was washed with water and brine, dried over Na₂SO₄, filtered, and evaporated to dryness. The residue was purified by flash chromatography on silica gel (2% MeOH in CH₂Cl₂) to deliver the title compound (0.67 g, 67%) as a yellow oil. ¹H NMR (300 MHz, CDCl₃) δ ppm 8.15 (s, 1H), 7.68 (d, $J = 8.7$ Hz, 1H), 7.48 (d, $J = 8.7$ Hz, 3H), 6.92 (d, $J = 8.7$ Hz, 2H), 4.20 (t, $J = 6.1$ Hz, 2H), 3.80 (s, 3H), 2.78 (t, $J = 6.1$ Hz, 2H), 2.33 (s, 3H).

(*E*)-Isopropyl But-2-enoylcarbamate (63). Isopropyl carbamate (30 g, 291 mmol) was charged to a 3 L Lara vessel, and dry THF (150 mL) added. (*2E*)-2-Butenoyl chloride (31.2 mL, 326 mmol) was added under nitrogen and the jacket cooled to –30 °C. When the solution temperature reached –17 °C, lithium *tert*-butoxide (655 mL, 655 mmol, 1 M in THF) was added by peristaltic pump over 2 h, keeping the reaction temperature between –10 °C and –18 °C. Once the addition was complete, the mixture was stirred for 30 min and brought to 0 °C. Et₂O (450 mL) and HCl (375 mL, 1 M aqueous solution) were added and the mixture brought to 20 °C with vigorous stirring. The stirring was stopped and the layers allowed to separate and the aqueous layer to run off. Brine (375 mL) was added and the mixture stirred vigorously. The stirring was stopped, and the layers were allowed to separate and the aqueous layer to run off. The organic layer was dried (MgSO₄), filtered, and evaporated to a brown oil (60 g). The mixture was loaded onto a 40+M Biotage silica column and eluted with CH₂Cl₂/EtOAc (1:1 → 0:1, 10CV). The product containing fractions were evaporated to dryness and loaded on to a 1500 g Rediseq Isco silica column and eluted with cyclohexane/EtOAc (0 → 40%, 17CV). The clean, product containing fractions were evaporated to an off-white solid (15.4 g, 29%). LCMS (method TFA): retention time 0.68 min, $[M + H]^+ = 172.0$. ¹H NMR (400 MHz, CDCl₃) δ ppm 1.30 (d, $J = 6.3$ Hz, 6H), 1.94 (dd, $J = 6.9, 1.6$ Hz, 3H), 4.94–5.06 (m, 1H), 6.87 (dd, $J = 15.4, 1.5$ Hz, 1H), 7.14 (dq, $J = 15.4, 6.9$ Hz, 1H), 7.35 (br s, 1H).

(*S*)-Isopropyl 3-((4-Bromophenyl)amino)butanoyl-carbamate (64). (*E*)-Isopropyl but-2-enoylcarbamate (63) (9.38 g, 54.8 mmol) was stirred in toluene (281 mL) under nitrogen and ((*R*)-BINAP)detriflatebis(acetonitrile)palladium(II) (3.35 g, 3.01 mmol) added. The catalyst formed a gummy ball, and the solution turned to an opaque yellow mixture and was stirred for 20 min. 4-Bromoaniline (14.14 g, 82 mmol) was added, the solution turned a clear light brown, and the gummy catalyst dissolved further. The mixture was stirred for 16 h. Similarly, a second batch of 1-methylethyl (*2E*)-2-butenoylcarbamate (8.51 g, 49.7 mmol) was stirred in toluene (255 mL) under nitrogen and ((*R*)-BINAP)detriflatebis(acetonitrile)palladium(II) (3.04 g, 2.73 mmol) added. The catalyst formed a gummy ball, and the solution turned to an opaque yellow mixture and was stirred for 20 min. 4-Bromoaniline (12.83 g, 74.6 mmol) was added, the solution turned a clear light brown, and the gummy catalyst dissolved further. The mixture was stirred for 16 h. The two reaction mixtures were combined and loaded on to a 1.5 kg Isco silica Rediseq column. The column was eluted with CH₂Cl₂/MeOH (0% → 0.5%, 19CV). The clean product containing fractions were evaporated to a pale-brown oil. The mixture was dried in a vacuum oven overnight at 40 °C to give a white solid (24.2 g, 67% overall). LCMS (method TFA) retention time = 0.91 min, $[M + H]^+ = 342.9$. Chiral HPLC: 92% ee (method: ~ 1 mg sample dissolved in EtOH/heptane (1 mL), 20 μ L injected on 4.6 mm i.d. \times 25 cm Chiralpak AD column (lot no. AD00CE-FE126)). Column eluted with 15% EtOH/heptane, $f = 1.0$ mL/min. UV detector wavelength = 215 nm). ¹H NMR (400 MHz, CDCl₃) δ ppm 1.26–1.35 (m, 9H), 2.90 (dd, $J = 16.0, 6.2$ Hz, 1H), 3.10 (dd, $J = 15.9, 5.8$ Hz, 1H), 3.86–3.94 (m, 1H), 3.94–4.06 (m, 1H), 4.92–5.03 (m, 1H), 6.51 (d, $J = 8.8$ Hz, 2H), 7.24 (d, $J = 8.8$ Hz, 2H), 7.44 (m, 1H).

Isopropyl ((2S,4R)-6-Bromo-2-methyl-1,2,3,4-tetrahydroquinolin-4-yl)carbamate (65). (*S*)-Isopropyl 3-((4-bromophenyl)amino)butanoylcarbamate (64) (17.9 g, 52.2 mmol) was taken up in EtOH (150 mL) and cooled to below –10 °C (internal temperature) in a CO₂/acetone bath. Sodium borohydride (1.381 g, 36.5 mmol) was added, followed by magnesium chloride hexahydrate (11.35 g, 55.8 mmol) in water (25 mL), keeping the temperature below –5 °C. The mixture was allowed to stir at <0 °C for 1 h then warmed to room temperature and stirred for 1 h. The resulting thick suspension was poured into a mixture of citric acid (25.05 g, 130 mmol), HCl (205 mL, 205 mmol, 1 M aqueous solution), and CH₂Cl₂ (205 mL). The biphasic mixture was stirred at room temperature for 1 h. The layers were separated and the organic layer dried over Na₂SO₄, filtered, and concentrated in vacuo to yield the product as a single *cis* isomer, a light-brown solid (14.1 g, 78%). LCMS (method formic):

retention time = 1.13 min, $[M + H]^+ = 327.2$ (99% purity). $^1\text{H NMR}$ (400 MHz, $\text{DMSO-}d_6$) δ ppm 1.14 (d, $J = 6.3$ Hz, 3H), 1.20 (d, $J = 6.3$ Hz, 3H), 1.23 (d, $J = 6.3$ Hz, 3H), 1.46 (q, $J = 11.9$ Hz, 1H), 1.88–1.97 (m, 1H) 3.40–3.51 (m, 1H), 4.69–4.79 (m, 1H), 4.78–4.88 (m, 1H), 6.48 (d, $J = 8.6$ Hz, 1H), 6.98 (s, 1H), 7.07 (dd, $J = 8.5, 1.9$ Hz, 1H), 7.42 (d, $J = 9.1$ Hz, 1H).

Isopropyl ((2*S*,4*R*)-1-Acetyl-6-bromo-2-methyl-1,2,3,4-tetrahydroquinolin-4-yl)carbamate (66). Isopropyl ((2*S*,4*R*)-6-bromo-2-methyl-1,2,3,4-tetrahydroquinolin-4-yl)carbamate (65) (14.1 g, 43.1 mmol) was taken up in CH_2Cl_2 (400 mL) under nitrogen at room temperature. Pyridine (10.46 mL, 129 mmol) followed by acetyl chloride (4.60 mL, 64.6 mmol) were added and the reaction stirred for 16 h. The reaction mixture was partitioned between EtOAc (2000 mL) and a saturated NaHCO_3 aqueous solution (800 mL). The organic layer was extracted and washed with water (1500 mL) and brine (1500 mL) and then dried over Na_2SO_4 , filtered, and concentrated in vacuo to yield a purple solid. The crude product was taken up in the minimum of dichloromethane and applied to a Companion XL column (330 g) and eluted with 12% EtOAc in cyclohexane for 1CV, then 12–63% EtOAc over 12 CV, then held at 63% for 4CV. The appropriate fractions were collected to afford the title product as an off-white solid (12.37 g, 78%). LCMS (method formic): retention time 1.03 min, $[M + H]^+ = 369.1$. $^1\text{H NMR}$ (600 MHz, $\text{DMSO-}d_6$) δ ppm 7.61 (br d, $J = 8.6$ Hz, 1H), 7.47 (dd, $J = 8.4, 2.4$ Hz, 1H), 7.29 (d, $J = 8.4$ Hz, 1H), 7.22 (d, $J = 2.4$ Hz, 1H), 4.83 (spt, $J = 6.2$ Hz, 1H), 4.66–4.58 (m, 1H), 4.40–4.33 (m, 1H), 2.44 (ddd, $J = 12.7, 8.5, 4.5$ Hz, 1H), 2.05 (s, 3H), 1.24 (dd, $J = 16.3, 6.1$ Hz, 6H), 1.21–1.16 (m, 2H), 1.02 (d, $J = 6.4$ Hz, 3H). $^{13}\text{C NMR}$ (150.9 MHz, $\text{DMSO-}d_6$) δ ppm 168.4 (s, 1C), 155.7 (s, 1C), 139.2 (s, 1C), 135.4 (br s, 1C), 129.6 (s, 1C), 128.1 (br s, 1C), 125.5 (s, 1C), 117.9 (s, 1C), 67.3 (s, 1C), 46.9 (br s, 1C), 46.6 (s, 1C), 39.6 (s, 1C), 22.5 (s, 1C), 22.0 (s, 2C), 21.2 (s, 1C). See Supporting Information Figure S4 for NMR spectra.

Separation of enantiomers: Chiralpak AD column, 20 μm particle size, internal diameter 75 mm, bed length 258 mm. Eluent 80:20 heptane:ethanol. Flow: 400 mL/min. Temperature: ambient. Injection volume: ~44 mL containing 4 g of compound 66 in 35:65 v/v heptane:ethanol. Run time: 4.5 min. Pure fractions containing the required first eluting enantiomer from all the injections were concentrated to dryness on a rotary evaporator to give product as a solid. This was slurried in heptane, stirred for 1 h at 20–25 $^\circ\text{C}$, filtered, washed on the filter with heptane, and dried under vacuum at 40 $^\circ\text{C}$ to give the product as a solid (89% recovery). HPLC analysis showed that the product contained <0.5% of the second eluting enantiomer. $[\alpha]_D^{20} = +281.1^\circ$ ($T = 20.7^\circ\text{C}$, 10 mm cell, $c = 0.508$ g/100 mL, EtOH).

Ethyl 4-((2*S*,4*R*)-1-Acetyl-4-((isopropoxycarbonyl)amino)-2-methyl-1,2,3,4-tetrahydroquinolin-6-yl)benzoate (67). Isopropyl ((2*S*,4*R*)-1-acetyl-6-bromo-2-methyl-1,2,3,4-tetrahydroquinolin-4-yl)carbamate (66) (53.47 g, 145 mmol), {4-[(ethoxy)carbonyl]phenyl}boronic acid (29.51 g, 152 mmol), and tetrakis-(triphenylphosphine)palladium (2.51 g, 2.17 mmol) were mixed in DME (500 mL) and the mixture treated with a 2N Na_2CO_3 aqueous solution (290 mL, 580 mmol). The mixture was degassed and then heated at 105 $^\circ\text{C}$ under nitrogen for 16 h. The mixture was then cooled to room temperature and was partitioned between EtOAc and water. The layers were separated, and the aqueous phase was extracted twice with EtOAc. The combined organics were washed with water and then brine, dried using a hydrophobic frit, and concentrated in vacuo. The residual gray–brown solid was dissolved in EtOAc and filtered through a plug of silica. The silica was washed with EtOAc, and the combined filtrate and washings were concentrated in vacuo to give a cream solid. This material was triturated with Et_2O , filtered, and the solid washed with a small volume of Et_2O . The solid was partially air-dried and then dried under vacuum at 40–50 $^\circ\text{C}$ to give the title compound (56.2 g, 89%) as a white solid, which was used in the next step without further purification. The filtrate and washings were concentrated in vacuo. The gummy brown residue obtained was triturated with Et_2O and the solvent removed in vacuo. The trituration with Et_2O was repeated. The solid obtained was collected by filtration, washed with Et_2O , and dried under vacuum at 40 $^\circ\text{C}$ to give another

batch of the title compound (1.7 g, 2.7%) as a very pale-gray solid, which was used in the next step without further purification. LCMS (method formic) retention time = 1.16 min, $[M + H]^+ = 439.16$. $^1\text{H NMR}$ (400 MHz, $\text{DMSO-}d_6$) δ 8.06 (d, $J = 8.3$ Hz, 2H), 7.80 (d, $J = 8.3$ Hz, 2H), 7.71 (d, $J = 8.8$ Hz, 1H), 7.65 (dd, $J = 1.8, 8.8$ Hz, 1H), 7.46 (m, 2H), 4.85 (spt, $J = 6.9$ Hz, 1H), 4.66 (m, 1H), 4.45 (m, 1H), 4.34 (q, $J = 7.1$ Hz, 2H), 2.47 (m, 1H), 2.10 (s, 3H), 1.35 (t, $J = 7.1$ Hz, 3H), 1.25 (t, $J = 6.9$ Hz, 6H), 1.19 (m, 1H), 1.06 (d, $J = 6.3$ Hz, 3H).

Ethyl 4-((2*S*,4*R*)-1-Acetyl-4-amino-2-methyl-1,2,3,4-tetrahydroquinolin-6-yl)benzoate (68). Ethyl 4-[(2*S*,4*R*)-1-acetyl-2-methyl-4-({[(1-methylethyl)oxy]carbonyl}amino)-1,2,3,4-tetrahydro-6-quinolinyl]benzoate (67) (25.33g, 57.8 mmol) was added to a ice-cold suspension of AlCl_3 (29.24 g, 219 mmol) in CH_2Cl_2 (450 mL), and the resulting solution was stirred at 0 $^\circ\text{C}$ for 20 min. A solution of NEt_3 (96 mL, 693 mmol) and MeOH (50 mL) was then added over approximately 2 min (initially dropwise and then faster after first third of the solution was used). The mixture was stirred for 30 min in the ice bath, then was diluted with EtOAc, filtered through Celite, and the residue washed with EtOAc. The residue was partitioned between EtOAc and a saturated sodium NaHCO_3 aqueous solution. The biphasic mixture was filtered through Celite, and the residue was washed with EtOAc. The residue was further washed with acetone and the acetone washings combined with the previous biphasic mixture. Most of the organics were concentrated in vacuo, and the aqueous residue was partitioned between EtOAc and water. The layers were separated, and the aqueous phase was extracted with EtOAc. The combined organic phases were washed with brine, dried using a hydrophobic frit, and concentrated in vacuo to give the title compound (14.7 g, 72%) as a cream solid which was used in the next step without further purification. The solid residue was rewashed with MeOH, and most of the MeOH was concentrated in vacuo. The residue was partitioned between EtOAc and water, and the layers were separated. The aqueous phase was extracted with EtOAc, and the combined organic phases were dried using a hydrophobic frit and concentrated in vacuo to give the title compound (5.3 g, 26%) as a cream solid, which was used in the next step without further purification. LCMS (method formic) retention time 0.73 min, $[M + H - \text{NH}_2]^+ = 337.3$. $^1\text{H NMR}$ (400 MHz, $\text{DMSO-}d_6$) δ 8.06 (d, $J = 8.3$ Hz, 2H), 7.87–7.91 (m, 3H), 7.63 (dd, $J = 2.0, 8.3$ Hz, 1H), 7.39 (d, $J = 8.3$ Hz, 1H), 4.62 (m, 1H), 4.36 (q, $J = 7.0$ Hz, 2H), 3.62 (m, 1H), 2.46 (m, 1H), 2.08 (s, 3H), 1.36 (t, $J = 7.0$ Hz, 3H), 1.19 (m, 1H), 1.06 (d, $J = 6.3$ Hz, 3H). NH_2 not observed.

Ethyl 4-((2*S*,4*R*)-1-Acetyl-4-[(4-chlorophenyl)amino]-2-methyl-1,2,3,4-tetrahydro-6-quinolinyl)benzoate (69). Ethyl 4-[(2*S*,4*R*)-1-acetyl-4-amino-2-methyl-1,2,3,4-tetrahydro-6-quinolinyl]benzoate (68) (24.6 g, 69.8 mmol), 1-bromo-4-chlorobenzene (26.7 g, 140 mmol), bis(dibenzylideneacetone)palladium (3.20 g, 5.56 mmol), and [2'-(dicyclohexylphosphanyl)-2-biphenyl]dimethylamine (Davephos, 2.19 g, 5.56 mmol) were mixed in toluene (450 mL), and the mixture was treated with sodium *t*-butoxide (7.38 g, 77 mmol). The resulting mixture was degassed and stirred at 70 $^\circ\text{C}$ under nitrogen for 24 h, then was cooled to room temperature and filtered through Celite. The residue was washed with toluene and then with Et_2O . The combined filtrate and washings were washed twice with water then twice with a 2 N HCl aqueous solution. The orange oil which precipitated was collected with the aqueous phase. The acid extracts were extracted with EtOAc, and the combined organics were washed with water and brine. This water and brine were combined with the acidic washes in order to recover the starting material (vide infra). The organic solution was further dried over MgSO_4 and concentrated in vacuo to give a dark-orange oil. This experiment was repeated, and the two residues hence obtained were combined for further purification. Purification of these combined residues by flash chromatography on silica gel (750 g column, 5–80% AcOEt in hexane) gave the title compound (16.5 g, 26% mean yield) as a pale-yellow foam. The impure fractions containing product were combined and concentrated in vacuo. Purification of this residue by flash chromatography on silica gel (330 g column, 5–80% AcOEt in hexane) gave the title compound (7.3 g, 11% mean yield) as a pale-brown foam. The combined acid

phases (vide supra) were basified using solid Na_2CO_3 and then were extracted three times with EtOAc. The combined organics were dried over MgSO_4 and combined with the same organic phases from the parallel experiment, then were concentrated in vacuo to give **69** (28.0 g, 57% average yield) as an orange foam which partially crystallized upon standing overnight. This material could be used in a repeat of this coupling without further purification. LCMS (method formic) retention time 1.35 min, $[\text{M} + \text{H} - \text{NHPHCl}]^+ = 337.23$. ^1H NMR (400 MHz, $\text{DMSO}-d_6$) δ 8.01 (d, $J = 8.6$ Hz, 2H), 7.69 (d, $J = 8.6$ Hz, 2H), 7.64 (dd, $J = 2.0, 8.1$ Hz, 1H), 7.47 (m, 2H), 7.12 (d, $J = 8.8$ Hz, 2H), 6.74 (d, $J = 8.8$ Hz, 2H), 6.30 (d, $J = 8.1$ Hz, 1H), 4.71 (m, 1H), 4.32 (q, $J = 7.1$ Hz, 2H), 4.28 (m, 1H), 2.62 (m, 1H), 2.15 (s, 3H), 1.33 (t, $J = 7.1$ Hz, 3H), 1.23 (m, 1H), 1.10 (d, $J = 6.1$ Hz, 3H).

FaSSIF Solubility. See Supporting Information, Supplementary Methods, for details of this high-throughput method to determine the solubility of compounds in fasted-state simulated intestinal fluid by precipitation.

ApoA1 Luciferase Assay. HepG2 cells were stably transfected with a plasmid encoding firefly luciferase under the control of the human ApoA1 promoter region (−1162, +232) and the 3′-UTR of the human ApoA-1 gene (+1037, +1091). ApoA1 potency was defined as the concentration of compound, resulting in a 70% increase in luciferase luminescence (ApoA1 Luc EC₁₇₀). See Supporting Information, Supplementary Methods. High correlation has been shown between ApoA1-luciferase reporter activity and ApoA1 protein secretion in HepG2 cells.²⁴

Recombinant Protein Binding Assays. The tandem bromodomain constructs of BRD2, BRD3, and BRD4 were screened in two formats. The FA (fluorescence anisotropy) assay measures displacement of a labeled benzodiazepine analogue of **1**, as previously described.⁴ The TR-FRET (time-resolved fluorescence resonance energy transfer) assay measures displacement of a tetra-acetylated biotinylated peptide. See Supporting Information, Supplementary Methods, for full details.

IL-6 PBMC and Whole Blood Assays. Human whole blood and peripheral blood mononuclear cells (PBMCs) purified from whole blood were incubated with LPS and varying concentrations of test compounds for 18–24 h. Samples were prepared, and inhibition of IL-6 was measured as described in Supporting Information, Supplementary Methods.

Thermal Shift Assay (T_m). Thermal shifts of bromodomains were analyzed on a FluoDiaT70 instrument. The temperature of the protein sample was ramped from 26/30 to 74 °C in the presence or absence of 100 μM of the ligand. Denaturation was visualized using 1:1000 dilution of a fluorescent Sypro orange dye in a buffer of PBS, 10% glycerol. The temperature was ramped at a rate of 1 °C/min and fluorescence readings taken every 1 °C. Bromodomains tested included ATAD2, BAZ2B, BRD2 (tandem bromodomains), BRD4 (N- and C-terminal and tandem bromodomains), CREBBP, PCAF, SMARCA2, SPI40, and TAF1 (tandem bromodomains). Results reported are the mean of at least two experiments.

Surface Plasmon Resonance (BIAcore) Analysis of Binding to BRD2, **3, and **4**.** BIAcore data of His6-tagged BRD2 (1–473), BRD3 (1–434), and BRD4 (1–477) was acquired and analyzed on a T100 BIAcore instrument at 25 °C. In all cases, a CM5 chip with ~5–12kU amine coupled protein immobilized on the dextran surface was used with a running buffer of 30 mM Hepes pH 7, 150 mM NaCl, 1 mM EGTA, Na₃. Compounds were titrated as a tripling dilution starting from 10 μM . Sensorgrams and binding curves were analyzed with BIAevaluation (GE Healthcare) using a 1:1 binding model. The equilibrium K_D was calculated using $\text{response} = \text{concentration} \times R_{\text{max}} / (\text{concentration} + K_D) + \text{offset}$. Example dose response fits are given in Supporting Information, Figure S2.

Isothermal Titration Calorimetry.³⁷ ITC titration of BRD4 was carried out using a Microcal VPITC in 50 mM Hepes, pH 7.5, 150 mM NaCl, at 25 °C. First, 9 μM His-tagged BRD4 (1–477) tandem bromodomain was placed in the cell and 200 μM ligand was titrated into this to achieve a final ligand:protein excess of ~4:1. The data was then fitted within Origin (Microcal version) to give the following

parameters: stoichiometry of 1.93, K_D of 4.4 ± 0.9 nM, ΔH −15.9 ± 0.08 kcal/mol, ΔS −15.2 cal/mol/deg.

ITC titration of CREBBP was carried out using a Microcal AutoITC200 in 50 mM Hepes, pH 7.4, 150 mM NaCl, at 25 °C. First, 44 μM of CREBBP bromodomain was placed in the cell, and 500 μM ligand was titrated into this to achieve a final ligand:protein excess of ~2.2:1. The data was then fitted within Origin (Microcal version) to give the following parameters: stoichiometry of 1.1, K_D of 6.3 ± 0.5 μM , ΔH −4.35 ± 0.08 kcal/mol, ΔS 9.2 cal/mol/deg.

X-ray Crystallography. General methods for the crystallography of the N-terminal bromodomain of Brd2 have been previously described.²⁹ The complexes of **28** and **47** were determined using *Escherichia coli* expressed His-tagged Brd2 (67–200). Specific details for each complex determined are given in Supporting Information, Supplementary Methods. For the C-terminal bromodomain of Brd2, *E. coli* expressed His-tagged Brd2-BD2 (338–473) was purified to homogeneity using standard protocols in a similar manner to the N-terminal bromodomain of Brd4 using His affinity capture, Tev protease cleavage, and gel filtration.⁷ See Supporting Information, Supplementary Methods, for full details. Ligand OMIT maps and refinement statistics are shown in Supporting Information Figure S3 and Table S5. Methods for the determination of the complex of **47** with the Brd4 N-terminal bromodomain and **48** with the Brd2 N-terminal bromodomain have previously been described.^{29,37}

Cytochrome P450 Inhibition and Time-Dependent Inhibition Studies. All cytochrome P450 inhibition studies were performed as described in Supporting Information, Supplementary Methods, at GlaxoSmithKline Medicines Research Centre (Stevenage, UK).

Hepatocyte Clearance. Intrinsic clearance studies were performed as described in Supporting Information, Supplementary Methods, at GlaxoSmithKline Medicines Research Centre (Ware, UK).

Permeability Assay. Artificial membrane permeability was measured as described in Supporting Information, Supplementary Methods.

Blood Protein Binding. All measurements of blood protein binding were performed as described in Supporting Information, Supplementary Methods, at GlaxoSmithKline Medicines Research Centre (Stevenage, UK).

Animal Studies. All animal studies were ethically reviewed and carried out in accordance with the GSK Policy on the Care, Welfare, and Treatment of Animals and European Directive 86/609. The rat PK study was performed at GSK Stevenage, UK, the dog PK study at GSK Ware, UK, the mouse PK studies at GSK Les Ulis, France, and the primate PK study at CIT, France. For all studies, the temperature and humidity were nominally maintained at 21 °C ± 2 °C and 55% ± 10%, respectively. There were no known contaminants in the diet or water at concentrations that could interfere with the outcome of the studies. See Supporting Information, Supplementary Methods.

Pharmacokinetics Studies. Diluted blood samples (1:1 with water) or plasma were extracted using protein precipitation with acetonitrile containing an analytical internal standard. An aliquot of the supernatant was analyzed by reverse phase LC-MS/MS using a heat assisted electrospray interface in positive ion mode. Samples were assayed against calibration standards prepared in control blood. PK parameters were obtained from the blood or plasma concentration–time profiles using noncompartmental analysis with WinNonlin Professional 4.1a (Pharsight, Mountain View, CA).

In Vivo Murine Efficacy Models. The effects of single-dose administration of compound **47** on LPS-induced PAI-1 RNA expression, and in a mouse model of septic shock, were determined as described in Supporting Information, Supplementary Methods.

■ ASSOCIATED CONTENT

📄 Supporting Information

Methods, bromodomain selectivity profile of **47**, BET binding curves of **47** by SPR, X-ray ligand density maps, NMR spectra, tables showing mean, standard deviation and number of test

occasions, thermal melting results for 47, receptor, transporter, and ion channel cross-screening of 47, X-ray data collection and refinement statistics. This material is available free of charge via the Internet at <http://pubs.acs.org>.

Accession Codes

The X-ray coordinates have been deposited with the Protein Data Bank. The codes are 4uyf (BRD2 N-terminal bromodomain with 47), 4uyg (BRD2 C-terminal bromodomain with 47), and 4uyh (BRD2 N-terminal bromodomain with 28).

AUTHOR INFORMATION

Corresponding Authors

*For P.B.: phone, +44 (0)20 8047 5000; fax, +44 1438 764486; E-mail, paul.a.bamborough@gsk.com.

*For R.K.P. (requests for material, research collaboration, etc.): phone, +44 1438 764303; E-mail: rabinder.prinjha@gsk.com.

Present Addresses

[¶]For R.G.: Galapagos SASU, 102 Avenue Gaston Roussel, 93230 Romainville, France.

*For C.S.: 71 Avenue Franklin Roosevelt, 94550 Chevilly Larue, France.

▲For O.M.: Institut de Recherche Servier, 11 rue des Moulineaux, 92150 Suresnes, France.

Notes

The authors declare no competing financial interest.

ACKNOWLEDGMENTS

We thank the DiscoveRx Corporation for BROMOScanSM selectivity screening. We thank Richard Upton (GlaxoSmithKline, Stevenage) for NMR support, Catherine Cartwright and James Clarke (GlaxoSmithKline, Ware) for in vitro preclinical developability profile information, and Nigel Parr and Iain Uings (GlaxoSmithKline, Stevenage) for leadership and helpful guidance given to the BET bromodomain program.

ABBREVIATIONS USED

AcK, acetyl-lysine; ApoA1, apolipoprotein A-1; BD, bromodomain; BET, bromodomain and extra-terminal; BRD2/3/4, bromodomain-containing protein 2/3/4; BZD, benzodiazepine; CREBBP, cAMP response element-binding binding protein; FA, fluorescence anisotropy; IL6, interleukin-6; LPS, lipopolysaccharide; NUT, nuclear protein in testis; THQ, tetrahydroquinoline; TR-FRET, time-resolved fluorescence resonance energy transfer

REFERENCES

(1) Toth, P. P. Cardiology patient page. The "good cholesterol": high-density lipoprotein. *Circulation* **2005**, *111*, e89–e91.
(2) Linsel-Nitschke, P.; Tall, A. R. HDL as a target in the treatment of atherosclerotic cardiovascular disease. *Nature Rev. Drug Discovery* **2005**, *4*, 193–205.
(3) Wong, N. C. Novel therapies to increase apolipoprotein AI and HDL for the treatment of atherosclerosis. *Curr. Opin. Invest. Drugs* **2007**, *8*, 718–728.
(4) Chung, C. W.; Coste, H.; White, J. H.; Mirguet, O.; Wilde, J.; Gosmini, R. L.; Delves, C.; Magny, S. M.; Woodward, R.; Hughes, S. A.; Boursier, E. V.; Flynn, H.; Bouillot, A. M.; Bamborough, P.; Brusq, J. M.; Gellibert, F. J.; Jones, E. J.; Riou, A. M.; Homes, P.; Martin, S. L.; Uings, I. J.; Toum, J.; Clement, C. A.; Boullay, A. B.; Grimley, R. L.; Blandel, F. M.; Prinjha, R. K.; Lee, K.; Kirilovsky, J.; Nicodeme, E. Discovery and characterization of small molecule inhibitors of the BET family bromodomains. *J. Med. Chem.* **2011**, *54*, 3827–3838.

(5) Mirguet, O.; Gosmini, R.; Toum, J.; Clément, C. A.; Barnathan, M.; Brusq, J.-M.; Mordaunt, J. E.; Grimes, R. M.; Crowe, M.; Pineau, O.; Ajakane, M.; Daugan, A.; Cutler, L.; Haynes, A. C.; Smithers, N. N.; Chung, C.; Bamborough, P.; Uings, I.; Lewis, A.; Witherington, J.; Parr, N.; Prinjha, R. K.; Nicodème, E. Discovery of epigenetic regulator I-BET-762: lead optimization to afford a clinical candidate inhibitor of the BET bromodomains. *J. Med. Chem.* **2013**, *56*, 7501–7515.

(6) *ClinicalTrials.gov*; National Library of Medicine: Bethesda, MD, August 30, 2014; <http://www.clinicaltrials.gov>.

(7) Nicodeme, E.; Jeffrey, K. L.; Schaefer, U.; Beinke, S.; Dewell, S.; Chung, C. W.; Chandwani, R.; Marazzi, I.; Wilson, P.; Coste, H.; White, J.; Kirilovsky, J.; Rice, C. M.; Lora, J. M.; Prinjha, R. K.; Lee, K.; Tarakhovsky, A. Suppression of inflammation by a synthetic histone mimic. *Nature* **2010**, *468*, 1119–1123.

(8) Florence, B.; Faller, D. V. You bet-cha: a novel family of transcriptional regulators. *Front Biosci.* **2001**, *6*, D1008–D1018.

(9) Belkina, A. C.; Denis, G. V. BET domain co-regulators in obesity, inflammation and cancer. *Nature Rev. Cancer* **2012**, *12*, 465–477.

(10) Chung, C. W. Small molecule bromodomain inhibitors: extending the druggable genome. *Prog. Med. Chem.* **2012**, *51*, 1–55.

(11) Chung, C. W.; Witherington, J. Progress in the discovery of small-molecule inhibitors of bromodomain–histone interactions. *J. Biomol. Screening* **2011**, *16*, 1170–1185.

(12) Muller, S.; Filippakopoulos, P.; Knapp, S. Bromodomains as therapeutic targets. *Expert Rev. Mol. Med.* **2011**, *13*, e29.

(13) Hewings, D. S.; Rooney, T. P.; Jennings, L. E.; Hay, D. A.; Schofield, C. J.; Brennan, P. E.; Knapp, S.; Conway, S. J. Progress in the development and application of small molecule inhibitors of bromodomain–acetyl-lysine interactions. *J. Med. Chem.* **2012**, *55*, 9393–9413.

(14) Adachi, K.; Endoh, J.; Fuhie, N.; Hamada, M.; Hikawa, H.; Ishibuchi, S.; Murata, M.; Oshita, K.; Sugahara, K.; Tanaka, M. Thienotriazolodiazepine compound and medicinal use thereof. WO2006129623A1, 2006.

(15) Miyoshi, S.; Ooike, S.; Iwata, K.; Hikawa, H.; Sugahara, K. Antitumor agent. WO2008-JP73864, 2008.

(16) Edwards, A. M.; Bountra, C.; Kerr, D. J.; Willson, T. M. Open access chemical and clinical probes to support drug discovery. *Nature Chem. Biol.* **2009**, *5*, 436–440.

(17) French, C. A. Pathogenesis of NUT midline carcinoma. *Annu. Rev. Pathol.* **2012**, *7*, 247–265.

(18) Filippakopoulos, P.; Qi, J.; Picaud, S.; Shen, Y.; Smith, W. B.; Fedorov, O.; Morse, E. M.; Keates, T.; Hickman, T. T.; Felletar, I.; Philpott, M.; Munro, S.; McKeown, M. R.; Wang, Y.; Christie, A. L.; West, N.; Cameron, M. J.; Schwartz, B.; Heightman, T. D.; La, T. N.; French, C. A.; Wiest, O.; Kung, A. L.; Knapp, S.; Bradner, J. E. Selective inhibition of BET bromodomains. *Nature* **2010**, *468*, 1067–1073.

(19) Mertz, J. A.; Conery, A. R.; Bryant, B. M.; Sandy, P.; Balasubramanian, S.; Mele, D. A.; Bergeron, L.; Sims, R. J., III. Targeting MYC dependence in cancer by inhibiting BET bromodomains. *Proc. Natl. Acad. Sci. U. S. A* **2011**, *108*, 16669–16674.

(20) Dawson, M. A.; Prinjha, R. K.; Dittmann, A.; Giotopoulos, G.; Bantscheff, M.; Chan, W. I.; Robson, S. C.; Chung, C. W.; Hopf, C.; Savitski, M. M.; Huthmacher, C.; Gudgin, E.; Lugo, D.; Beinke, S.; Chapman, T. D.; Roberts, E. J.; Soden, P. E.; Auger, K. R.; Mirguet, O.; Doehner, K.; Delwel, R.; Burnett, A. K.; Jeffrey, P.; Drewes, G.; Lee, K.; Huntly, B. J.; Kouzarides, T. Inhibition of BET recruitment to chromatin as an effective treatment for MLL-fusion leukaemia. *Nature* **2011**, *478*, 529–533.

(21) Delmore, J. E.; Issa, G. C.; Lemieux, M. E.; Rahl, P. B.; Shi, J.; Jacobs, H. M.; Kasttris, E.; Gilpatrick, T.; Paranal, R. M.; Qi, J.; Chesi, M.; Schinzel, A. C.; McKeown, M. R.; Heffernan, T. P.; Vakoc, C. R.; Bergsagel, P. L.; Ghobrial, I. M.; Richardson, P. G.; Young, R. A.; Hahn, W. C.; Anderson, K. C.; Kung, A. L.; Bradner, J. E.; Mitsiades, C. S. BET bromodomain inhibition as a therapeutic strategy to target c-Myc. *Cell* **2011**, *146*, 904–917.

- (22) Ott, C. J.; Kopp, N.; Bird, L.; Paranal, R. M.; Qi, J.; Bowman, T.; Rodig, S. J.; Kung, A. L.; Bradner, J. E.; Weinstock, D. M. BET bromodomain inhibition targets both c-Myc and IL7R in high-risk acute lymphoblastic leukemia. *Blood* **2012**, *120*, 2843–2852.
- (23) Puissant, A.; Frumm, S. M.; Alexe, G.; Bassil, C. F.; Qi, J.; Chanthery, Y. H.; Nekritz, E. A.; Zeid, R.; Gustafson, W. C.; Greninger, P.; Garnett, M. J.; McDermott, U.; Benes, C. H.; Kung, A. L.; Weiss, W. A.; Bradner, J. E.; Stegmaier, K. Targeting MYCN in neuroblastoma by BET bromodomain inhibition. *Cancer Discovery* **2013**, *3*, 308–323.
- (24) Mirguet, O.; Lamotte, Y.; Donche, F.; Toum, J.; Gellibert, F.; Bouillot, A.; Gosmini, R.; Nguyen, V. L.; Delannee, D.; Seal, J.; Blandel, F.; Boullay, A. B.; Boursier, E.; Martin, S.; Brusq, J. M.; Krysa, G.; Riou, A.; Tellier, R.; Costaz, A.; Huet, P.; Dudit, Y.; Trottet, L.; Kirilovsky, J.; Nicodeme, E. From ApoA1 upregulation to BET family bromodomain inhibition: discovery of I-BET151. *Bioorg. Med. Chem. Lett.* **2012**, *22*, 2963–2967.
- (25) Seal, J.; Lamotte, Y.; Donche, F.; Bouillot, A.; Mirguet, O.; Gellibert, F.; Nicodeme, E.; Krysa, G.; Kirilovsky, J.; Beinke, S.; McCleary, S.; Rioja, L.; Bamborough, P.; Chung, C. W.; Gordon, L.; Lewis, T.; Walker, A. L.; Cutler, L.; Lugo, D.; Wilson, D. M.; Witherington, J.; Lee, K.; Prinjha, R. K. Identification of a novel series of BET family bromodomain inhibitors: binding mode and profile of I-BET151 (GSK1210151A). *Bioorg. Med. Chem. Lett.* **2012**, *22*, 2968–2972.
- (26) Wyspianska, B.; Bannister, A. J.; Barbieri, I.; Nangalia, J.; Godfrey, A.; Calero-Nieto, F. J.; Robson, S.; Rioja, L.; Li, J.; Wiese, M.; Cannizzaro, E.; Dawson, M. A.; Huntly, B.; Prinjha, R. K.; Green, A. R.; Gottgens, B.; Kouzarides, T. BET protein inhibition shows efficacy against JAK2V617F driven neoplasms. *Leukemia* **2013**, *28*, 88–97.
- (27) Bailey, D.; Jahagirdar, R.; Gordon, A.; Hafiane, A.; Campbell, S.; Chatur, S.; Wagner, G. S.; Hansen, H. C.; Chiacchia, F. S.; Johansson, J.; Krimbou, L.; Wong, N. C.; Genest, J. RVX-208: a small molecule that increases apolipoprotein A-I and high-density lipoprotein cholesterol in vitro and in vivo. *J. Am. Coll. Cardiol.* **2010**, *55*, 2580–2589.
- (28) McLure, K. G.; Gesner, E. M.; Tsujikawa, L.; Kharenko, O. A.; Attwell, S.; Campeau, E.; Wasiak, S.; Stein, A.; White, A.; Fontano, E.; Suto, R. K.; Wong, N. C.; Wagner, G. S.; Hansen, H. C.; Young, P. R. RVX-208, an inducer of ApoA-I in humans, is a BET bromodomain antagonist. *PLoS. One* **2013**, *8*, e83190.
- (29) Chung, C. W.; Dean, A. W.; Woolven, J. M.; Bamborough, P. Fragment-based discovery of bromodomain inhibitors part 1: inhibitor binding modes and implications for lead discovery. *J. Med. Chem.* **2012**, *55*, 576–586.
- (30) Fish, P. V.; Filippakopoulos, P.; Bish, G.; Brennan, P. E.; Bunnage, M. E.; Cook, A. S.; Federov, O.; Gerstenberger, B. S.; Jones, H.; Knapp, S.; Marsden, B.; Nocka, K.; Owen, D. R.; Philpott, M.; Picaud, S.; Primiano, M. J.; Ralph, M. J.; Sciammetta, N.; Trzuppek, J. D. Identification of a chemical probe for bromo and extra C-terminal bromodomain inhibition through optimization of a fragment-derived hit. *J. Med. Chem.* **2012**, *55*, 9831–9837.
- (31) Bamborough, P.; Diallo, H.; Goodacre, J. D.; Gordon, L.; Lewis, A.; Seal, J. T.; Wilson, D. M.; Woodrow, M. D.; Chung, C. W. Fragment-based discovery of bromodomain inhibitors part 2: optimization of phenylisoxazole sulfonamides. *J. Med. Chem.* **2012**, *55*, 587–596.
- (32) Hewings, D. S.; Wang, M.; Philpott, M.; Fedorov, O.; Uttarkar, S.; Filippakopoulos, P.; Picaud, S.; Vuppasetty, C.; Marsden, B.; Knapp, S.; Conway, S. J.; Heightman, T. D. 3,5-Dimethylisoxazoles act as acetyl-lysine-mimetic bromodomain ligands. *J. Med. Chem.* **2011**, *54*, 6761–6770.
- (33) Hewings, D. S.; Fedorov, O.; Filippakopoulos, P.; Martin, S.; Picaud, S.; Tumber, A.; Wells, C.; Olcina, M. M.; Freeman, K.; Gill, A.; Ritchie, A. J.; Sheppard, D. W.; Russell, A. J.; Hammond, E. M.; Knapp, S.; Brennan, P. E.; Conway, S. J. Optimization of 3,5-dimethylisoxazole derivatives as potent bromodomain ligands. *J. Med. Chem.* **2013**, *56*, 3217–3227.
- (34) Gehling, V. S.; Hewitt, M. C.; Vaswani, R. G.; Leblanc, Y.; Côté, A.; Nasveschuk, C. G.; Taylor, A. M.; Harmange, J.-C.; Audia, J. E.; Pardo, E.; Joshi, S.; Sandy, P.; Mertz, J. A.; Sims, R. J.; Bergeron, L.; Bryant, B. M.; Bellon, S.; Poy, F.; Jayaram, H.; Sankaranarayanan, R.; Yellapantula, S.; Srinivasamurthy, N. B.; Birudukota, S.; Albrecht, B. K. Discovery, design and optimization of isoxazole azepine BET inhibitors. *ACS Med. Chem. Lett.* **2013**, *4*, 835–840.
- (35) Zhao, L.; Cao, D.; Chen, T.; Wang, Y.; Miao, Z.; Xu, Y.; Chen, W.; Wang, X.; Li, Y.; Du, Z.; Xiong, B.; Li, J.; Xu, C.; Zhang, N.; He, J.; Shen, J. Fragment-based drug discovery of 2-thiazolidinones as inhibitors of the histone reader BRD4 bromodomain. *J. Med. Chem.* **2013**, *56*, 3833–3851.
- (36) Bellosa, S.; Paoletti, R.; Corsini, A. Safety of statins: focus on clinical pharmacokinetics and drug interactions. *Circulation* **2004**, *109*, III50–III57.
- (37) Wyce, A.; Ganji, G.; Smitheman, K. N.; Chung, C.-W.; Korenchuk, S.; Bai, Y.; Barbash, O.; Le, B.; Craggs, P.; McCabe, M. T.; Kennedy-Wilson, K. M.; Sanchez, L. V.; Gosmini, R. L.; Parr, N.; McHugh, C. F.; Dhanak, D.; Prinjha, R. K.; Auger, K. R.; Tummino, P. J. BET inhibition silences expression of MYCN and BCL2 and induces cytotoxicity in neuroblastoma tumor models. *PLoS. One* **2013**, *8*, e72967.
- (38) Marshall, J. C. Why have clinical trials in sepsis failed? *Trends Mol. Med.* **2014**, *20*, 195–203.
- (39) Filippakopoulos, P.; Picaud, S.; Mangos, M.; Keates, T.; Lambert, J. P.; Baryte-Lovejoy, D.; Felletar, I.; Volkmer, R.; Muller, S.; Pawson, T.; Gingras, A. C.; Arrowsmith, C. H.; Knapp, S. Histone recognition and large-scale structural analysis of the human bromodomain family. *Cell* **2012**, *149*, 214–231.
- (40) Demont, E. H.; Gosmini, R. Tetrahydroquinoline derivatives as bromodomain inhibitors and their preparation and use in the treatment of cancer, autoimmune and inflammatory diseases. WO2010-EP66701, 2010.
- (41) Damon, D. B.; Dugger, R. W.; Hubbs, S. E.; Scott, J. M.; Scott, R. W. Asymmetric synthesis of the cholesterol ester transfer protein inhibitor torcetrapib. *Org. Process Res. Dev.* **2006**, *10*, 472–480.